2022

Role of Host Restriction Factors on Porcine Reproductive and Respiratory Syndrome Virus (PRRSV) Replication

Pratik Katwal
South Dakota State University, pratik.katwal@jacks.sdstate.edu

ROLE OF HOST RESTRICTION FACTORS ON PORCINE REPRODUCTIVE AND RESPIRATORY SYNDROME VIRUS (PRRSV) REPLICATION

BY

PRATIK KATWAL

A dissertation submitted in partial fulfillment of the requirements for the

Doctor of Philosophy

Major in Biological Sciences

Specialization in Microbiology

South Dakota State University

2022

DISSERTATION ACCEPTANCE PAGE

Pratik Katwal

This dissertation is approved as a creditable and independent investigation by a candidate for the Doctor of Philosophy degree and is acceptable for meeting the dissertation requirements for this degree. Acceptance of this does not imply that the conclusions reached by the candidate are necessarily the conclusions of the major department.

Xiuqing Wang
Advisor Date

Radhey Kaushik
Department Head Date

Nicole Lounsbery, PhD
Director, Graduate School Date

This work is dedicated to my daughter Angelina.

ACKNOWLEDGMENTS

First and foremost, I want to thank my parents for their constant support and encouragement. I am very grateful to my wife, Bijayata Singh Kunwar, who supported me throughout my PhD study. We are very blessed to have baby Angelina in our life.

Above all, I want to sincerely thank my doctoral advisor, Dr. Xiuqing Wang for guiding me in my research. I am indebted to her for accepting me in her lab as a doctoral student. I am thankful to her for mentoring me in my research. I would also like to take this opportunity to thank Dr. Michael Hildreth, whose expertise in confocal microscopy helped me tremendously in my experiments. Also, I want to thank Dr. Eric Nelson and Craig Welbon for providing MARC-145 cells, PRRSV 23983 virus stock, and SDOW17 antibody. I want to thank Dr. Radhey Shyam Kaushik for providing the needed reagents for my experiments and for his help with my PhD plan of study. I would also like to thank Dr. Shitao Li of Tulane University for providing the IFITM3 and ZMPSTE24 plasmids. I greatly appreciate Dr. Liping Gu of the SDSU functional genomics core facility for helping me with lab equipment set up. I want to sincerely thank the department of Biology and Microbiology for supporting me with graduate assistantship. I also want to thank my lab partners, Shamiq Aftab and Theresah Amponsah for helping me with molecular techniques. This study was partly supported by Agriculture and Food Research Initiative Competitive Grant no. 2021-67016-34460 from the USDA National Institute of Food and Agriculture, USDA NIFA Hatch (grant #1000514), Hatch (SD00H660-19) and Hatch Multi State (SD00R656-16), (Grant #1010908), and South Dakota Agricultural Experiment Station. I am grateful for their support.

TABLE OF CONTENTS

ABBREVIATIONS

%: Percentage

ALRs: AIM2-like receptor

BHK-21: Baby Hamster kidney cells

CARD: Caspase activation and recruitment domain

CD163: Cluster of Differentiation 163

CD169: Cluster of Differentiation 169

cGAS: Cyclic GMP-AMP synthase

CH25H: Cholesterol 25-hydroxylase

CIL: Conserved intracellular loop

CMV: Cytomegalovirus

CTD: C-terminal domain

DMV: Double membrane vesicle

dsRNA: Double stranded RNA

E: Envelope

EBV: Epstein-Barr virus

EEA1: Early endosome antigen-1

ER: Endoplasmic reticulum

F-actin: Filamentous actin

FLIM: Fluorescence lifetime imaging microscopy

GAF: Gamma-interferon activation factor

GAS: Gamma-activated sequence

GP: Glycoprotein

HA: Hemagglutinin

HCMV: Human Cytomegalovirus

HCoV-OC43: Human coronavirus OC43

HCV: Hepatitis C virus

HGPS: Hutchinson-Gilford progeria syndrome

HIV: Human immunodeficiency virus

hMPV: Human metapneumovirus

Hpi: Hours post-infection

HPV-16 E6: Human papilloma virus type 16 E6

IAV: Influenza A virus

IFA: Immunofluorescence assay

IFITM3: Interferon induced transmembrane protein 3

IFNAR: Interferon alpha receptor

IFNLR1: Interferon Lambda Receptor 1

IFN-α: Interferon alpha

IL-10R2: Interleukin-10 receptor 2

IMD: Intra-membrane domain

IRF: Interferon regulatory factor

ISG: Interferon stimulated gene

ISGF3: Interferon stimulated gene factor 3

ISRE: Interferon-stimulated response element

JAK: Janus Kinase

kDa: Kilodalton

LAMP-1: Lysosomal-associated membrane protein 1

M: Membrane protein

mAb: Monoclonal Antibody

MAVS: Mitochondrial antiviral-signaling protein

MDA5: Melanoma differentiation-associated protein 5

MEF: Mouse embryonic fibroblast

mRNA: Messenger RNA

mTOR: Mammalian target of Rapamycin

Mx: Myxovirus resistance protein

N protein: Nucleocapsid protein

NF-κβ: Nuclear factor kappa-light-chain-enhancer of activated B cells

Nsp: Non-structural protein

NTD: N-terminal domain

ORF: Open reading frame

OSBP: Oxysterol-binding protein 1

PAM: Porcine alveolar macrophage

PAMP: Pathogen associated molecular pattern

PK-15: Porcine kidney 15 cell line

PKR: Protein kinase R

Pp: Polyprotein

PRR: Pattern recognition receptor

PRRSV: Porcine reproductive and respiratory syndrome virus

RdRp: RNA dependent RNA polymerase

RIG-I: Retinoic acid-inducible gene I

RLR: RIG-I-like receptors

ROS: Reactive Oxygen species

RTC: Replication and transcription complex

SOCS: Suppressor of cytokine signaling

SRCR: Scavenger receptor Cysteine rich domain

ssRNA: Single stranded RNA

STAT: Signal transducer and activator of transcription

STING: Stimulator of interferon genes

TMD: Transmembrane domain

TNT: Tunneling nanotube

TRIM: Tripartite motif

TYK2: Tyrosine-Kinase 2

VAPA: Vesicle associated membrane protein-A

vATPase: Vacuolar ATPase

vRNP: Viral ribonucleoprotein

ZAP: Zinc finger antiviral protein

ZMPSTE24: Zinc metallopeptidase STE24

LIST OF FIGURES

LIST OF TABLES

ABSTRACT

ROLE OF HOST RESTRICTION FACTORS ON PORCINE REPRODUCTIVE AND RESPIRATORY SYNDROME VIRUS (PRRSV) REPLICATION

PRATIK KATWAL

2022

In this study, the role of IFITM3 on PRRSV replication was studied in vitro by expressing exogenous IFITM3 in MARC-145 cells. An average of 31% reduction in PRRSV N protein expression and an average of 5.4 fold decrease in virus titer in the supernatant were observed in IFITM3 overexpressing cells as compared to vector control cells at 24 hours post infection (hpi). Moreover, there was a positive correlation between interferon-induced IFITM3 up-regulation and reduced PRRSV replication. To determine the role of endogenous IFITM3 in PRRSV replication, siRNA induced knockdown of IFITM3 was employed. RT-PCR validated the successful silencing of IFITM3 in MARC-145 cells, with an average knockdown of 50%. PRRSV RNA copies were 1.28-fold higher in IFITM3 silenced cells as compared to control silencing, suggesting that knockdown of endogenous IFITM3 only slightly enhanced PRRSV replication. Taken together, these results suggest antiviral role of IFITM3 against PRRSV in vitro. In this study, we tested if the antifungal drug Amphotericin B restores PRRSV replication in IFITM3 overexpressing MARC-145 cells. Amphotericin B only partially restored PRRSV replication as confirmed by flow cytometry. Interestingly, more colocalization of PRRSV with early endosome marker was observed at 3 hpi (37.9%) than at 1 hpi (23.8%) and 6 hpi (31.8%). To further investigate the stage of PRRSV infection restricted by IFITM3 over-expression, colocalization study was performed at 3 and 24 hpi. Our results

showed that IFITM3 expressing cells were positive for PRRSV at both 3 and 24 hpi. The percentage of IFITM3 positive cells with positive PRRSV staining was significantly higher at 3 hpi as compared to 24 hpi. Collectively, our data suggest that IFITM3 may restrict PRRSV via multiple post-entry mechanisms.

The role of restriction factor, ZMPSTE24, on PRRSV replication was also studied. The ZMPSTE24 exerted antiviral effect against PRRSV as confirmed by both ZMPSTE24 overexpression and silencing experiments. A reduced expression of PRRSV N protein by approximately 3% and a 146-fold decrease in virus titer in the supernatant in the ZMPSTE24 overexpressing cells compared to vector control were observed. To further determine the role of endogenous ZMPSTE24 in PRRSV replication, we performed siRNA induced silencing of ZMPSTE24 in MARC-145 cells. RT-PCR validated highly successful silencing of ZMPSTE24, with an average knockdown of 74%. Knockdown of endogenous ZMPSTE24 slightly affected PRRSV replication, as only 1.2 fold increase in PRRSV RNA copies was observed. To study the stage of PRRSV infection impeded by ZMPSTE24, colocalization study was performed at 3 and 24 hpi. There were no significant differences in the number of PRRSV positive cells or total viral RNA copies between the vector control and ZMPSTE24 over-expressing cells at 3 hpi. The colocalization of PRRSV with ZMPSTE24 was significantly higher at 3 hpi as compared to 24 hpi, suggesting that ZMPSTE24 does not affect PRRSV entry into endosomes and restriction occurs after 3 hpi. Taken together, our results suggest that IFITM3 and ZMPSTE24 likely restrict PRRSV at multiple post-entry steps.

Chapter 1: Literature Review

1.1 An overview of Porcine Reproductive and Respiratory Syndrome Virus (PRRSV)

1.1.1 PRRSV genome, structure, and replication

Porcine reproductive and respiratory syndrome virus (PRRSV) belongs to the family *Arteriviridae* in the order *Nidovirales* [66]. Within this order, the family *coronaviridae* is also included. In contrast to the coronaviruses family, the known members of the *Arteriviridae*, which includes PRRSV, equine arteritis virus, and three other members, show narrow host range and commonly infect a single animal species [66, 161]. PRRSV is an enveloped virus, spherical or oval shaped, with a positive (+) sense, single stranded RNA (ssRNA) genome [32, 90]. It has a diameter of 45-65 nm and accommodates the nucleocapsid (N) protein that is about 20-35 nm in diameter [32]. The molecular weight of N protein is about 15 kDa and anti-N monoclonal antibodies (mAbs) have been shown to recognize both the conserved and variable epitopes within the PRRSV N protein [32, 98, 161]. The North American and European strains were identified using the anti-N (mAb) [161]. The PRRSV RNA genome is approximately 15 kb in length and contains eleven open reading frames (ORFs) of which the replicase associated ORF1a and b are the largest and encode the viral polymerase [90]. The replicase associated polyproteins pp1a and pp1ab are encoded by the ORFs 1a and 1b and are translated from the genomic mRNA [90]. These polyproteins are subsequently processed to produce 14 non-structural proteins (nsps). The ORF1a encodes transmembrane (TM) domains. The RNA-dependent RNA polymerase (RdRp) is encoded by the ORF1b [90]. On the other hand, the subgenomic mRNAs from the ORFs 2-7 encode the minor envelope proteins (GP2a, GP3, GP4, E, and ORF5a), major

envelope proteins (GP5 and M), and the nucleocapsid protein (N) [66]. Therefore, eight structural proteins are encoded by the subgenomic mRNAs [66]. The mature non-structural proteins synthesized from the pp1a and pp1ab polyproteins assemble to form the replication and transcription complex (RTC) which leads to the synthesis of full length complementary minus (-) strand by the viral RdRp [38, 66]. The continuous (-) strand synthesis serves as a template for genome replication while the discontinuous (-) strand synthesis serves as a template for the synthesis of subgenomic mRNA [38]. The PRRSV non-structural proteins nsp2 and nsp7 have been show to localize to the perinuclear region in the area of endoplasmic reticulum which forms modifications leading to the double membrane vesicles (DMVs), the site for assembly of the RTC [38, 66, 103]. The PRRSV genome is packaged within the nucleocapsid (N). During the process of budding, PRRSV becomes enveloped and is then released from the cell by exocytosis.

1.1.1.1 An overview of PRRSV receptor and entry factors

Several studies attempted to identify the principal receptor for PRRSV attachment and entry [127]. Early studies indicated that the intermediate filament protein, vimentin may be an important factor in PRRSV attachment and entry [19, 71]. Vimentin is expressed on the MARC-145 cells and anti-vimentin antibody inhibited PRRSV entry and subsequent infection [71]. Also, expression of simian vimentin protein rendered non-permissive cells susceptible to PRRSV. However, these studies did not conclusively demonstrate the role of vimentin in supporting productive virus replication. Another important candidate in the search for PRRSV receptor was porcine sialoadhesin (CD169). Sialoadhesin is a membrane glycoprotein in the siglec family of sialic acid binding lectins [144]. Monoclonal antibody against sialoadhesin blocked PRRSV infection in porcine

alveolar macrophage (PAM) [33]. Transfection of the non-permissive PK-15 cells with porcine sialoadhesin enabled virus internalization. However, no productive virus replication could be observed due to block in the virus fusion step [135]. Also, heparan sulfate was found to be an important factor in PRRSV entry. However, both sialoadhesin and heparan sulfate are not expressed on MARC-145 cells [33]. Eventually, CD163, belonging to the scavenger receptor cysteine-rich (SRCR) superfamily was identified as the principal receptor for PRRSV [19]. CD163 is principally expressed in the differentiated macrophages, with low level of expression in undifferentiated cells [19, 37, 111, 144]. In this regard, its aberrant expression in MARC-145 cells renders these cells susceptible to PRRSV [144]. Transfection of CD163 cDNA in the non-permissive cell lines such as the baby hamster kidney (BHK-21) cells not only rendered them susceptible to PRRSV infection, but also resulted in productive virus replication [19].

The SRCR family of proteins recognizes a wide variety of ligands and functions as pattern recognition molecules by binding to various bacterial and viral pathogens [37, 144]. CD163 is a type 1 transmembrane protein consisting of nine highly conserved extracellular domains, each consisting of about 110 amino acids, also called SRCR domains [37, 144]. CD163 expressed in macrophages has been best characterized as a receptor that binds the hemoglobin-heptaglobin complex, thereby clearing these complexes by endocytosis [37, 46, 48]. This protects tissues from oxidative damage that could potentially result from the free hemoglobin released by lysis of red blood cells [48]. CD163 is a group B SRCR protein and consists of eight cysteine residues per domain, with the exception of domain eight. The loop 5-6 region of the SRCR 5 has been shown to be highly conserved across different mammalian species [144]. The SRCR 5 domain

has been shown to be the main site of interaction with PRRSV for infection [132, 144]. Expression of CD163 on porcine macrophages has been shown to correlate with infection with African Swine Fever Virus [110]. CD163 recycles between plasma membrane and endosome, unlike the sialoadhesin CD169 which is mainly expressed at the plasma membrane. CD163 colocalizes with PRRSV in the early endosomes and PRRSV interaction with both CD169 and CD163 has been shown to be important in the infection of PAMs [130, 131]. Non-permissive cells co-expressing CD169 and CD163 were shown to have enhanced virus infectivity as compared to cells expressing CD163 alone [130]. Therefore, CD169 is the internalization receptor while CD163 is critical for virus uncoating within the endosomes.

1.1.1.2 Receptor mediated endocytosis

Initial attachment of PRRSV membrane (M) protein to the heparan sulfate molecules on PAMs is followed by virus internalization [28]. This occurs through interaction of PRRSV GP5/M proteins with sialoadhesins which leads to the internalization of PRRSV into clathrin-coated vesicles [96, 129]. The receptor mediated endocytosis is dependent on the interaction of PRRSV with CD163 which occurs within the early endosomes [19, 131]. This leads to the uncoating of PRRSV within the acidic (low pH) environment. Studies have suggested that the process of PRRSV entry into endosomes and subsequent uncoating in MARC-145 occurs in a manner similar to PAMs [73]. The endosomes are characterized by unique pH; as virus trafficking occurs through early endosome to late endosome, there is a progressive increase in acidity of the organelles. Early endosomes have a pH of 6-6.5, while late endosomes and lysosomes have pH values in the range of 5-6 to 4.6-5 respectively [131]. Treatment of PAMs with bases such as NH_4Cl and chloroquine was shown to block virus uncoating as viruses were

trapped within the vesicles, indicating that virus uncoating requires fusion with low pH endosomes [96]. The Rab family of small GTPases are often used as markers for the identification of endosomes. These proteins are important in the regulation of the endocytic pathways, chiefly clathrin-coated-vesicle-mediated transport [152]. Rab5 and its effector, early endosome antigen (EEA1) can be used to study the colocalization of PRRSV within early endosomes [131]. Late endosomes/lysosomes are characterized by the LAMP-1 marker. In primary alveolar macrophages, colocalization of PRRSV was observed with the EEA1 marker. However, little or no colocalizaton was observed with the LAMP-1 marker [131]. These findings suggest that entry of PRRSV may occur through early endosomes.

1.1.1.3 pH dependent fusion of viruses within the endocytic pathway

Viruses whose fusion in the endosomes is dependent on pH are most sensitive to IFITM mediated restriction. IFITM proteins, chiefly IFITM2 and IFITM3 are located within early and late endosomes and restrict viruses within these compartments by inhibiting fusion of host cell membrane with the virus membrane [121]. IFITM has been tested against several viruses for its antiviral activity and majority of these viruses are enveloped. As viruses are trafficked through the endocytic pathway, they encounter progressively acidic environments within the low pH endosomes [121]. IFITM3 has been shown to inhibit West Nile virus, vesicular stomatitis virus, etc. that fuse at pH greater than 6. These viruses are inhibited within the early endosome, which has a pH varying between 6 to 6.5 [47, 121, 142]. On the other hand, Influenza virus, Dengue virus, etc. that fuse at pH below 6 are inhibited by IFITM3 within the late endosomes where the pH varies between 5-5.5 [16, 57, 121]. IFITM1 is expressed mainly at the plasma membrane and has been shown to inhibit viruses whose fusion is independent of pH, or whose

fusion is further upstream of the endocytic pathway where the pH is notably higher [83, 92]. Therefore, IFITMs restrict several enveloped viruses at different stages of cellular trafficking. The fusion mechanism of most of these viruses is triggered at a specific pH. These findings suggest that in general, IFITM mediated restriction is imposed at the stage of cellular entry. This is consistent with findings of several studies which suggest that IFITM directly or indirectly interferes with cell-virus fusion and a number of models have been proposed to explain the mechanism of IFITM mediated virus restriction [104].

1.1.2 PRRSV infectivity

PRRSV exhibits very narrow host range and pigs are the only known natural host of PRRSV. PRRSV shows very restricted tropism in the natural host, infecting cells of the monocyte lineage, principally the fully differentiated porcine alveolar macrophages (PAMs) [19]. In cell culture, the African green monkey kidney cells MA-104 and its derivate, MARC-145 cells are fully susceptible to PRRSV, supporting productive virus replication [19, 70]. Besides these cell lines, PRRSV has also been reported to infect VERO cells and CL-2621 [12, 74, 118]. However, although VERO cells support successful attachment and internalization similar to MARC-145 cells, they do not support successful virus replication [74]. At present, MARC-145 cells are the most commonly used cell line for PRRSV propagation and infectivity studies in vitro [19, 90].

1.1.3 Clinical signs, pathogenesis, and transmission

In the beginning, PRRSV was identified as a pathogen causing reproductive disease in gilts and sows and respiratory disease in young pigs. Initially, it was reported to have caused outbreaks in North America and Western Europe [68, 161]. Clinical diseases due to PRRSV infection include anorexia, still born, early farrowing, and abortion [68, 161]. However, clinical outcomes have been reported to vary among herds

and in general lead to subclinical infections [161]. Nursery pigs infected with PRRSV often show chronic disease along with secondary bacterial or viral co-infections [161]. Studies have shown that fetuses are susceptible to PRRSV during the whole gestation period [25, 32, 68, 161]. Congenital PRRSV infections have been shown experimentally [32, 161]. Reproductive loss and infertility in sows is an important characteristic of the disease. Although fetuses of the PRRSV inoculated sows remain susceptible throughout the entire gestation period under experimental conditions, exposure of sows to PRRSV in the field leads to reproductive failure in the late gestation period [68, 76, 161]. This has been show to correlate well with the presence of the macrophages in the endometrium and placenta that express the principal PRRSV receptor, CD163, in addition to sialoadhesin [68]. Therefore, transplacental infection is reported mostly in the late gestation period due to PRRSV replication in the target cells. Intranasal inoculation of sows with PRRSV results in efficient replication of PRRSV in the respiratory tract, leading to viremia that then eventually spreads to the endometrium and placenta, thereby causing apoptosis of cells during the late gestation period [68].

PRRSV infection can be divided into three stages: acute infection, persistence, and extinction [90]. In the acute stage, PRRSV principally infects macrophages in the respiratory tract. Typically, viremia occurs at 12 hours post infection [90, 161]. Although gross lesions are only observed occasionally in the lungs of experimentally inoculated animals, microscopic lesions have been reported in lungs, lymph nodes, and blood vessels. In the persistence stage, viremia subsides along with the absence of the obvious signs of clinical disease. Virus replication mainly occurs in the lymphoid organs at this stage, thereby leading to increased spread of virus via oral-nasal secretions [90]. In the

extinction phase, virus is completely cleared off, which may take up to 250 days after infection [90]. Overall, the degree and extent of the clinical respiratory disease could be affected by the age of the infected animal, virulence of the PRRSV strain, and the antibody dependent enhancement of infection [149, 161]. The presence of sub-optimal or sub-neutralizing antibodies against PRRSV leads to exacerbation of the disease outcome in the infected animals [161]. The presence of cross-reactive antibodies in the animals enhances the infection by increased uptake of virus by macrophages and has been demonstrated under experimental conditions [149, 161].

Two genotypes of PRRSV are known. The North American genotype appeared in the late 1980s and this was followed by the European genotype which appeared in the early 1990s [145]. There is only about 55-70% nucleotide similarity between the two genotypes [2, 97]. PRRSV has a high degree of transmissibility [11, 161]. Most of the swine producing areas of the world today have reported PRRSV infection, with global distribution spanning across North America, Europe and Asia [30, 161]. Serological studies showed that PRRSV entered the swine population in Iowa in the mid 1980s, and increase in prevalence of PRRSV was reported each year thereafter [11, 161]. PRRSV causes severe respiratory disease in young pigs and reproductive failure in sows [90]. Depending on the PRRSV strain, pigs in some farms showed subclinical infections, while other farms showed severe respiratory or reproductive disease in pigs [90]. Also, the emergence of highly pathogenic PRRSV strains has caused significant economic loss to the pork industry not only in North America, but also in Europe and Asia [53, 67, 93, 128]. Several experimental studies have shown that PRRSV can play important role in porcine respiratory disease complex and is often responsible for exacerbating the

pulmonary disease conditions when co-infection with other bacterial or viral pathogens occurs [21]. The suppression of immune response by PRRSV has also been well studied, which may explain the susceptibility of the host to infection with other secondary bacterial or viral pathogens.

The dominant neutralizing epitope has been shown to be located in the PRRSV GP5, along with identification of epitopes on both M and GP4 proteins [89, 100, 133]. PRRSV glycoprotein cluster GP2a-GP3-GP4 interacts with the principal receptor CD163 during infection [27]. Suppression of interferon production in cells infected with PRRSV due to its interference with the IFN components is one of the major factors responsible for the delayed antibody response. PRRSV may antagonize the IFN response by inhibiting the IFN regulatory factors (IRFs) whose activation is critical for the IFN activity [90]. Likewise, glycan shielding masks the neutralizing epitopes, thereby allowing evasion of the antiviral response [89]. The N-glycans in both GP5 and GP3 have been shown to be important in impeding the neutralizing antibody response [36, 137]. PRRSV strains differ in their N glycosylation patterns [36]. These may also lead to persistence of virus in pigs [89].

PRRSV is a highly infectious virus, requiring very low infectious dose to produce infection in the animal host [161]. PRRSV is very sensitive to external environment as it is an enveloped virus. It is generally a labile virus and is inactivated rapidly at temperatures above 37^{o}C [32, 105]. Although aerosol formation has been suggested to be the primary route of virus transmission, it has been very difficult to demonstrate aerosol transmission under experimental conditions [161]. On the other hand, several studies have shown PRRSV transmission by direct contact [32]. Acutely infected animals are

reported to infect other animals by direct contact. These animals can transmit virus for up to 15 weeks post infection [161]. In nursery pigs, direct contact may be a major route of PRRSV transmission [32].

1.2 Innate immunity

1.2.1 A brief overview of Interferon response

Interferons play a crucial role in the control of virus infection. Upon infection of cells, the interferon pathway is activated which then alarms the cells of foreign invasion [109, 126]. This eventually leads to the clearance of pathogens. The early description of interferon reported the role of a newly identified substance that inhibited influenza virus infection [58]. Further studies identified interferons as small proteins produced by cells upon recognition of the pathogen [80]. The innate immune sensors, called pattern recognition receptors (PRRs) recognize pathogen-associated molecular patterns (PAMPs) expressed on microbes. This begins a cascade of signaling leading to IFN production [115]. Interferons are grouped into three different classes and are defined based on their receptor complexes. There are three interferon types and each type is known to perform distinct functions within cells. The most commonly studied IFN in regard to antiviral immunity are the Type I and Type II IFNs [115]. Moreover, while many viruses induce IFN response in infected cells, some viruses interfere with IFN and downregulate IFN synthesis as a means of evading antiviral immunity.

1.2.1.1 Summary of the three classes of Interferon

Type I interferon in humans consists of IFNα, IFNβ, IFNε, IFNκ, and IFNω. These interferons signal through binding to the IFN alpha receptor 1 and 2 heterodimer (IFNAR1 and IFNAR2) [109, 115]. The Type I IFN receptors are expressed on most nucleated cells [56]. Although most cells can produce and respond to IFNα and IFNβ, the

predominant IFN alpha producing cells are the plasmacytoid dendritic cells [87, 115]. IFNɤ is the only known member of the type II IFN family whereas the most recently discovered type III IFN includes a number of members, principally the IFN λ1, IFN λ2, and IFN λ3, and a recently identified IFN λ4 [56, 115]. Type II interferons act through the IFN gamma receptor heterodimer (IFNɤ1 and IFNɤ2) while type III interferons act through the low affinity receptor subunit, interleukin 10 receptor 2 (IL-10R2); and the high affinity receptor subunit, IFN λ receptor 1 (IFNLR1) heterodimer [56, 115]. Type II IFN receptors have a broad tissue distribution and most cell types respond to type II IFN. The IFN gamma is mainly produced by immune cells [109]. In contrast, the type III IFN receptor IFNLR1 is mainly restricted to the epithelial cells as a result of which many cell types respond poorly to type III IFN [56].

1.2.1.2 An overview of Interferon signaling

Upon binding to their respective receptor complexes, the signaling of Type I and Type III interferons converge at the STAT1/STAT2 phosphorylation [115]. Briefly, phosphorylation and activation of Janus Kinase JAK1 and Tyrosine Kinase (TYK2) in the cytoplasmic domain which occurs as a result of conformational change in the IFN receptor chain upon IFN binding, leads to the subsequent phosphorylation of Tyrosine residues [26, 56, 115]. This is followed by the recruitment of signal transducers and activators of transcription (STAT1 and 2) which then undergo phosphorylation at specific tyrosine residues and associate to form a STAT1/STAT2 heterodimer [26, 56]. This heterodimer then associates with the Interferon regulatory factor 9 (IRF9) forming the Interferon stimulated gene factor 3 (ISGF3) which is then translocated to the nucleus, leading to the activation of interferon stimulated genes (ISGs) [56, 115]. Binding of IFN gamma (Type II interferon) leads to the phosphorylation and activation of the JAK1 and

JAK2 with the subsequent recruitment and phosphorylation of STAT1 homodimer [109]. This forms the IFN gamma activation factor (GAF) which is translocated to the nucleus leading to expression of ISGs [115]. The ISGF3 binds to the DNA gene sequence on the IFN stimulated response elements (ISRE) while GAF binds to the DNA on the gamma-activated sequence (GAS) elements [109, 115]. Ultimately, both processes lead to the antiviral state through the production of various antiviral proteins. Of the seven known STAT proteins in mammals, STAT1 and STAT2 are predominantly involved in signaling through the IFN receptor complex [115]. Therefore, JAK-STAT signaling pathway and its regulation-the central component of IFN signaling-are responsible for the antiviral effector functions.

1.2.2 An overview of the innate immune response and its relevance to PRRSV

PRRSV is sensitive to type I Interferon treatment. Primary PAM cells pretreated with Interferon alpha (IFN-α) inhibits PRRSV replication [18]. Upon entry of virus into host cells, the recognition of pathogen associated molecular patterns (PAMPs) by pattern recognition receptors (PRRs) activates innate immune signaling. For instance, the recognition of double stranded RNA (dsRNA) by Rig-1-like receptors (RLRs) leads to inflammatory response through NF-κβ nuclear transcription factor or through the activation of interferon response involving the phosphorylation and nuclear translocation of interferon regulatory factors (IRF3 and IRF7) [115]. The interferon then binds to the interferon receptor on the cell surface, thereby activating the expression of various IFN stimulated genes (ISGs). This is dependent on the JAK/STAT signaling pathway [115]. Unlike swine influenza virus infection which leads to upregulation of IFN-α, PRRSV modulates the IFN response, thereby antagonizing the antiviral response [90, 134]. Suppression of IFN-α response correlates with enhanced PRRSV replication. Stimulation

of cells with low level of IFN-α has been shown to enhance PRRSV infectivity [29]. One study showed that although PRRSV induced the transcription of IFN-α, very low amount of this cytokine could be detected in supernatant, suggesting that PRRSV interferes with either the post-transcriptional or translational step of IFN-α synthesis [155]. PRRSV nonstructural proteins nsp1, 2, 4, and 11 have been shown to downregulate the IFN-α response [24, 90]. The nsp1α and nsp1β proteins interfere with IRF3 phosphorylaton and nuclear translocation, thereby inhibiting the IFN synthesis [14]. Further, PRRSV nsp1β blocks the nuclear translocation of the IFN-stimulated gene factor 3 (ISGF3), a heterotrimer of STAT1, STAT2, and IRF9. This leads to the inhibition of expression of ISGs important in the antiviral response [102]. MARC-145 cells infected with PRRSV followed by IFN-α treatment showed significantly low ISG15 and ISG56 expression as compared to mock infected cells [102].

1.2.2.1 A summary of PRRSV and ISGs

Interferon does not induce antiviral state on its own. Rather, this is dependent on the activity of various ISGs that are induced upon interferon treatment. Protein kinase R (PKR) is a well-studied classical ISG that is induced upon interferon treatment. Upon virus infection, it is activated in cells following recognition of double stranded RNA (dsRNA) [146]. The antiviral state is induced as a result of stall in cellular translation following phosphorylation of the eukaryotic translation initiation factor, eIF2α [148]. Studies suggest that PKR exerts antiviral effect via inhibition of PRRSV gene transcription [108]. Interestingly, PRRSV is also known to interfere with PKR activation in porcine alveolar macrophages (PAMs) and this may help to evade the antiviral response during early infection [148]. However, another study has shown that PKR plays a pro-viral role during PRRSV infection [140].

The role of many ISGs in PRRSV replication has not been extensively studied. Although IFITM3 has been shown to inhibit several enveloped viruses, very limited information on the role of this restriction factor on replication of the members of arterivirus family is available. One study has reported the antiviral role of the interferon stimulated gene ISG12A in PRRSV replication in vitro [60]. ISG12A localized in the mitochondria and interfered with cell cycle regulation [60]. Another important restriction factor is the interferon stimulated gene ISG20 that inhibits several RNA viruses [34, 143, 160]. ISG20, a 3'-5' exonuclease specifically acting on ssRNA, was shown to upregulate the expression of several antiviral gene transcripts, including a subset of ISGs [143]. However, the role of this restriction factor in PRRSV replication has not been characterized.

1.2.2.2 IFITM3 and PRRSV infection

A recent study has demonstrated the antiviral role of IFITM3 on PRRSV replication. Overexpression of IFITM3 in MARC-145 cells or porcine alveolar macrophage (PAMs) showed significant reduction in the PRRSV titer [153]. Further, knockdown of endogenous IFITM3 enhanced virus replication [153]. IFITM3 did not inhibit the attachment or entry into the endocytic vesicles [153]. In contrast to a previous study that showed that PRRSV enters into early endosomes only, this study showed that PRRSV is first trafficked through early endosome, then to late endosomes and lysosomes [131, 153, 156]. PRRSV was shown to colocalize with IFITM3 positive endosomes and lysosomes and IFITM3 restricted PRRSV by preventing membrane fusion [153]. Further, altered accumulation of cholesterol within the endosomes was shown to be important in the IFITM3 mediated restriction of PRRSV [153].

1.2.3 An overview of Interferon stimulated genes (ISGs) and their activation

Pattern recognition receptors (PRRs) are specialized at detecting pathogens through their recognition of pathogen associated molecular patterns or PAMPs [1, 125]. The PRRs broadly recognize different classes of pathogens. These can be divided into either the non-cytosolic PRRs or the cytosolic PRRs. The cytosolic PRRs recognize either singe stranded or double stranded viral RNA or DNA. The cytosolic PRRs such as the RIG-1 and MDA5 recognize viral nucleic acids, i.e. single stranded RNA (ssRNA) or double stranded RNA (dsRNA) and the differential recognition of dsRNA is dependent on the length of the dsRNA. The RIG-1 receptors recognize 5' triphosphate RNA, a non-self RNA signature [1, 125]. On the other hand, the cyclic GMP-AMP synthase (cGAS) and the AIM2-like receptors (ALRs) detect viral DNAs. In addition, detection of foreign RNA also activates the endoribonuclease RNaseL that cleaves the foreign RNA with the production of additional PAMPs that further stimulates the Rig-1 like receptors (RLRs) [56]. Another important sensor of foreign RNA is the protein kinase R or PKR that also plays an important role in activating the innate immune response against pathogens [95]. Overall, the detection and activation of the PRRs upon recognition of the viral nucleic acids activates the downstream signaling through the adaptor proteins- stimulator of IFN genes (STING) and mitochondrial antiviral signaling protein (MAVS) at the endoplasmic reticulum (ER) and mitochondrial membrane interface [56, 115, 125]. This occurs as a result of the interaction of caspase activation and recruitment (CARD) domain on the RLRs with the mitochondrial adaptor molecules. Activation of STING/MAVS leads to phosphorylation and activation of the IFN response factors 3 or 7 (IRF3 or IRF7) which form homodimers [56, 125]. In addition, phosphorylation with ubiquitination and degradation of IκB activates the nuclear transcription factor NF-κB. The activated

IRF3/IRF7 and NF-κB are translocated to the nucleus where binding to specific promoters leads to the induction of IFN synthesis as well as activation of a subset of ISGs [56, 115]. Activation of IRF3, IRF7 and NF-κB is necessary to induce the expression of IFNβ from the IFNβ promoter [56]. In addition, some of the IRFs and PRRs may also be activated that enhances pathogen detection and antiviral immune response. IFN binds to the IFN receptor complex on the cell surface thereby activating the signaling through the JAK-STAT pathway [115]. This eventually leads to the induction of various ISGs with the subsequent induction of the antiviral response.

1.2.3.1 Negative regulation of IFN signaling by ISGs

Cells enter a state of IFN desensitization in which the IFN response is negatively regulated [78]. This allows cells to recover from the IFN signaling whereby cells return to the normal state before IFN sensitization [115]. On the other hand, IFN dysregulation leads to continued IFN response leading to various autoimmune diseases. The negative regulation of IFN can occur either through cell intrinsic mechanisms or by the action of various ISGs [115]. The two important ISGs that negatively regulate the IFN signaling are the suppressor of cytokine signaling (SOCS) and the ubiquitin specific peptidase 18 (USP18). The SOCS family of proteins acts as kinase inhibitors. They bind to phosphorylated tyrosine residues which inhibit STAT binding [115]. The SOCS1 and SOCS3 function as pseudosubstrates for the receptor-associated JAKs. The SOCS proteins play an important role in early desensitization and depending on the cell type, their basal level of expression may vary, which determines the level of responsiveness of cells to IFN treatment [115].

Long-term or sustained desensitization to IFN signaling is maintained by USP18. The covalent linkage of the IFN induced ubiquitin-like protein (ISG15) to proteins is

referred to as ISGylation [115]. The peptidase activity of USP18 is necessary for the removal of the ISG15 congujates, a process known as deISGylation [10]. Consequently, USP18 knockdown significantly enhances type I IFN responsiveness thereby making the cells resistant to virus infection as demonstrated in animal model studies [115]. The long-term desensitization of IFN signaling by USP18 is dependent on binding of the USP18 to the intracellular domains of the IFN alpha receptor 2 (IFNAR2). This leads to conformational change in the extracellular domain of the IFNAR2 which inhibits the binding of the low affinity type I IFN, i.e. IFN alpha [10, 115]. However, the binding of IFN beta, a high affinity type I IFN, is unhindered and therefore, responsiveness to IFN beta is unaffected despite the binding of USP18 to IFNAR2. Also, since USP18 binds specifically to the IFNAR2, it is unable to affect the type II IFN signaling [115].

1.2.4 Interferon induced transmembrane protein 3 (IFITM3) family

The members of the interferon induced transmembrane family (IFITM) of proteins are important restriction factors that are constitutively expressed in many cell types [6, 115]. Although most cell types are known to express IFITM proteins, their basal level of expression may vary across cell types. Interferon (IFN) treatment potently induces IFITM expression in cells [6]. In humans, IFITM1, IFITM2, and IFITM3, together with IFITM5 form a gene cluster [6]. The IFITM1, 2, and 3 proteins are commonly known as the antiviral IFITMs as they are known to restrict a number of enveloped viruses. The IFITM5 is associated with osteoblast and is non-antiviral in function. In addition, humans also have IFITM10 gene that is located outside of the IFITM gene cluster and its function is not known yet [6]. IFITM1 is mostly expressed in the plasma membrane while IFITM2 and IFITM3 are expressed in the early and late endosomes and are known to inhibit a number of enveloped viruses by preventing their

release into the cytosol [121]. In cell culture, IFITM knockout mouse embryonic fibroblasts (MEFs) were shown to be highly susceptible to Influenza A virus (IAV) infection. Likewise, in vivo studies showed that IFITM knockout mice were highly susceptible to the pathogenic H1N1 strain (A/PR/8/34) [4, 16, 35].

1.2.4.1 Summary of IFITM domains and membrane topology

IFITM proteins consist of five domains: the N-terminal domain (NTD), intramembrane domain (IMD), conserved intracellular loop (CIL), transmembrane domain (TMD), and C-terminal domain (CTD) [6, 121]. The current model of IFITM membrane topology classifies it as a type II transmembrane protein. The NTD (intracellular) faces cytosol while the CTD (extracellular), together with the CIL, faces the lumen of the endoplasmic reticulum/endosome [6, 121]. Both IFITM2 and IFITM3 contain YXXF motifs [62]. The Tyr20 (Y20) in the NTD is highly conserved in IFITM2 and IFITM3 and is important for the internalization into endosomes [6, 61, 104]. There are four lysines in the IFITM that can be ubiquitinated, one of which is located in the NTD (K24) [151]. The Lys24 in the NTD is most efficiently ubiquitinated by Lys48 ubiquitin linkage as compared to the other lysines (located at the conserved intracellular loop). Ubiquitination at K24 position promotes degradation and has been shown to affect the antiviral activity of IFITM [6, 151]. Ubiquitination therefore regulates IFITM expression and protein turnover. While two highly conserved cysteine residues are located in the IMD, a poorly conserved cysteine residue is located at the junction between the CIL and the TMD [6, 121]. Substitution of cysteine with alanine has been shown to inhibit antiviral activity [6, 64]. These cysteines are palmitoylated, containing covalently linked palmitic acid and have been shown to be important in the subcellular localization

of IFITM [6, 150, 151]. The palmitoylation of Cys72 residue plays an especially important role in the IFITM mediated virus restriction [6, 150, 151].

Broadly, based on the membrane topology of the IFITM proteins, several key features in the context of antiviral functions can be highlighted. As a type II transmembrane protein, the amphipathic helix of the hydrophobic domain 1 and the transmembrane helix of the hydrophobic domain 2 are critical for the antiviral activity of IFITM [5, 119]. Multimerization of IFITM is considered essential for antiviral activity. The IFITM proteins have been shown to induce positive (+) curvature as visualized from the cytosolic side [51, 119]. Also, studies have indicated that interaction of IFITM with other proteins, chiefly the zinc metalloprotease, ZMPSTE24, may be important for its antiviral function [84, 119]. In addition, IFITM proteins also modulate the activity of the vacuolar ATPase (v-ATPase) [119, 141]. This is important because it provides yet another indirect mechanism for virus inhibition by trapping them within the acidic endolysosomal compartments and targeting them for degradation. In addition, some studies have shown that IFITM may increase cholesterol incorporation within the endosomal membrane [3]. These studies suggest that not only IFITM inhibits viruses by direct mechanism, but also various indirect mechanism of inhibition may be involved. The most widely accepted model is the tough membrane model in which IFITM directly alters the physical properties of the membrane. Recent studies with IAV using live cell imaging have shown that IFITM3 inhibits fusion of viruses by partitioning into virus positive endosomes [124]. When A549 cells were transduced with GFP-fused IFITM3, the IFITM3 expressing cells were protected from IAV infection [124]. IFITM3 associated

with domains where cell-virus fusion occurs, thereby imposing a block in the virus entry step [51].

1.3 IFITM3 mediated antiviral activity

Several cell-cell fusion studies have provided key insights as to how IFITMs perform their antiviral functions [83]. These studies are based on the cell membrane expression of IFITM and viral envelop proteins, whereby the ability of IFITM to inhibit fusion of the envelop proteins is studied. A recent cell-cell fusion assay using human metapneumovirus (hMPV) fusion (F) protein-based luciferase activity demonstrated that IFITM3 protein significantly inhibits membrane fusion mediated by hMPV [91]. These assays suggest that IFITM3 may alter the physical properties of the membrane, thereby rendering the cell-virus fusion process unfavorable.

1.3.1 Virus-host membrane fusion step: the main target for IFITM3

Fusion is a critical step in virus entry. For example, following attachment to the cell surface receptor and internalization, the influenza A virus (IAV) undergoes trafficking through the endocytic pathway. Within the late endosomes, the low pH environment triggers a conformational change in the IAV hemagglutinin (HA) protein, a major viral envelope protein, thereby allowing the fusion of viral membrane with the endosomal membrane [39]. Precisely, this occurs through the fusion of the outer leaflet of the viral membrane with the leaflet of the endosomal membrane on the luminal side. The outcome of this process is the formation of a hemifusion intermediate. This is followed by the fusion of the inner leaflet of the viral membrane with cytoplasmic leaflet of the endosomal membrane, forming a stable fusion pore [104, 120]. This enables the release of the viral ribonucleoprotein (vRNP) into the cytosol. The IFITM3 protein imposes a block in the IAV fusion step and as a result, the cytosolic entry of the vRNP and its

eventual transport into the nucleus is inhibited [39, 104]. IFITM3 has been shown to partially co-localize with the late endosomal and lysosomal markers- Rab7 and LAMP-1 respectively, thus placing it in the optimum position for inhibiting IAV, which mainly enters through late endosomes [39]. Similarly, in a recent study of classical swine fever virus infection, IFITM proteins have been shown to colocalize with Rab5, Rab7, and LAMP-1 endosomal markers [82].

1.3.2 The tough membrane model

According to the tough membrane model, IFITM may increase the rigidity of the membrane thereby preventing the process of cell-virus fusion and this can occur in a number of ways. Viruses such as HIV-1 and HCV require interaction with one or more co-receptors following the attachment of specific virus protein to the receptors. First, upon initial binding to the receptor, the pair moves laterally until it encounters the co-receptors. This triggers the fusion peptide insertion [104]. IFITMs decrease membrane fluidity, thereby preventing the lateral movement of the receptor complex. The intramembrane domain 1 (IM1) of IFITM that integrates into the outer (cytoplasmic) leaflet of the endosomal membrane has been shown to be important in this process [104]. Other viruses such as IAV require the clustering of the HA receptors. The two HAs with their fusion peptides inserted into the host membrane, move through the membrane until they coalesce. This allows the formation of fusion pore. IFITM proteins restrict this movement and inhibit fusion pore formation [59, 104]. Not only does the interaction of the IM1 domain of IFITM decreases membrane fluidity, but also induces a curvature that makes fusion pore formation energetically unfavorable [51, 104]. Several studies support the tough membrane model for IFITM3 mediated virus restriction. Studies using fluorescence lifetime imaging microscopy (FLIM) have shown that IFITM3

overexpression leads to decrease in host cell membrane fluidity with the restriction in lateral movement of plasma membrane proteins [83, 86]. In addition, the IFITM proteins have been proposed to concentrate in the receptor enriched regions in the cell membrane called lipid rafts where virus binds to receptors [3, 15, 104]. Therefore, even a relatively low level of expression of IFITM may inhibit viruses by altering the cell membrane [104]. Overall, IFITMs restrict virus entry by making the membrane less fluid and increases stiffness in the cytoplasmic leaflet of the endosomal membrane [51].

In addition to the direct mechanism, IFITMs may also indirectly inhibit viruses by modulating the endosomal acidification. Studies on IAV support this model in which it was shown that IFITM overexpression leads to expansion of acidified organelles [39]. In another study, it was shown that the IAV variants that fuse at a higher pH were more resistant to the IFITM mediated restriction. This allows the viruses to escape the more acidic, late endosomal compartments where IFITM3 are predominantly expressed [45]. In addition, co-immunoprecipitation studies have shown direct association between the IFITM3 proteins and the vATPase [141]. The IFITM3 proteins have also been implicated in interfering with the lipid homeostasis; IFITMs have been shown to increase the accumulation of cholesterol in the late endosome, thereby imposing a block in virus fusion. The IFITMs bind to the vesicle associated membrane protein-A (VAPA) and competes with the oxysterol binding protein (OSBP)-a regulator of IFITM trafficking-for VAPA binding which increases cholesterol content in the endosomes [3, 147].

Amphotericin B is an antifungal drug that increases membrane fluidity by forming ion leak channels [6]. Amphotericin B has been shown to restore membrane fluidity thereby reversing the effect of IFITM3 on virus restriction [86, 91]. The

Amphotericin B drug may disrupt a higher order complex of IFITMs [6]. This could be a possible explanation for its effect on membrane fluidity. Amphotericin B treatment has been shown to fully restore infection of hMPV, IAV, etc. in cells overexpressing IFITM3 [86, 91].

1.3.3 Diverse roles of ISGs

1.3.3.1 Effects of host restriction factors on virus infection

Upon binding of enveloped virus to cell surface receptor, it either enters into the cell by fusion with cell membrane or becomes internalized in the vesicles for trafficking within the endosomes, a process known as receptor mediated endocytosis. Within the acidic endosomes, virus fusion is mediated thereby allowing virus uncoating and release of the genome. In general, this occurs as a result of low pH triggered conformational change in the viral envelope proteins and insertion of the fusion peptide into the cell membrane [54]. Replication and transcription of the virus is followed by packaging of the genome, then assembly and release. Each of these steps within the virus life cycle can be a potential target for the host's restriction factors. In recent years, a wide variety of restriction factors have been identified [23, 117, 119]. Restriction factors inhibit virus at various stages of virus infection. Restriction factors such as the Cholesterol-25-Hydroxylate (CH25H) and IFITM1 are known to inhibit fusion of enveloped virus with the host membrane, thereby blocking virus entry [115]. IFITM3 blocks host-virus membrane fusion within endosomes and inhibits virus uncoating. The trapped virus is then degraded within the highly acidic endolysosomal compartments [104]. In addition, incorporation of IFITM into the newly released virion membranes inhibits the subsequent fusion of virus and infection of new host cells [23]. Myxovirus resistance (Mx) proteins prevent transport of viral DNA or vRNPs into nucleus. The human ortholog MxA protein

blocks the release of influenza vRNP in the cytoplasm. ZAP prevents translation of viral RNA by targeting them for degradation. Viperin inhibits virus budding from the host cell while Tetherin prevents the release of virus from the cell [23]. However, viruses have also evolved with countermeasures to evade the host restriction factor that allows successful infection of host cells [72]. Some viruses have co-opted the host restriction factors by hijacking them for their own benefit [157].

Table 1.1 Summary of important cellular restriction factors and their antiviral roles [23].

Restriction factor	**Stage of virus life cycle**
CH25H	entry
IFITM1,2,3	entry, fusion
Mx	Nuclear import, transcription
ZAP	translation
TRIM25	replication
Tetherin	egress
Viperin	transcription
ZMPSTE24	entry

1.3.3.2 Summary of ISG profiles and their diverse functions

Stimulation of the ISGs is a major step in the antiviral response. Signaling through the JAK-STAT pathway eventually leads to the activation of various ISGs. The ISGs can be grouped into various categories depending on their antiviral roles or their activity as regulators of the interferon signaling pathway. Broadly, there are three types of ISGs: antiviral effectors, positive regulators and negative regulators [117]. One of the

most widely studied IFN stimulated genes is the MX family of proteins [136]. There are several ISGs that are important for antiviral effector functions and include IFITM3, CH25H, TRIM, Viperin, Tetherin, etc. [23]. Some of the classical IFN induced antiviral ISGs include MX1, OAS and PKR [116]. Broadly, these ISGs inhibit viruses at various stages of replication cycle. On the other hand, there are also ISG types that function as negative regulators of IFN signaling [116]. SOCS and USP18 both interfere with the JAK-STAT pathway thereby inhibiting IFN signaling. There are several positive regulators of IFN signaling and includes various PRRs, cGAS, RNAseL, PKR, IRF3, 7, and 9 [115]. IRF1 is an important positive regulator which upon expression can directly stimulate the production of various ISGs. It is important to note that IRF1 is able to induce expression of hundreds of ISGs in the absence of IFN and STAT1 signaling [115]. Therefore, IFN regulatory factors function as important component that regulate the IFN signaling pathway and the production of ISGs. Upon sensing of virus nucleic acids by cytosolic PRRs, the activated IRFs then induce IFN gene expression. The IFN signals through the JAK-STAT pathway to induce the antiviral state. While many ISGs inhibit viruses, some ISGs have been shown to enhance virus replication. Characterization of ISG profile against six highly pathogenic viruses showed that a cluster of ISGs enhanced virus replication [116, 117]. Some viruses have co-opted the ISGs for their own benefit. For example, HCoV-OC43 virus replication is enhanced by upregulation of IFITM3 although IFITM3 is known to potently inhibit several enveloped viruses [157]. Viperin is an important antiviral effector against many viruses [115]. However, HCMV viruses encode for proteins that co-opts viperin and disrupts actin cytoskeleton by modulating ATP production [116]. This enhances HCMV infection, indicating that HCMV hijacks

ISG for successful infection. Therefore, for such viruses, upregulation of specific ISG does not correlate with antiviral activity. While some ISGs promote IFN signaling either by directly acting on the JAK-STAT pathway or on the IFN regulatory factors, there are other ISGs which act as negative regulators and target the PRRs, IRFs or the components of the JAK-STAT pathway [85, 116].

Studies have demonstrated redundancies in the ISG antiviral activity as mice defective in classical antiviral pathways such as Mx1 and PKR are still able to generate antiviral response [159]. In HCV infected patients, upregulation of a unique set of 36 signature ISGs in the liver upon IFN treatment has been show to correlate with reduction in HCV viral load [17]. Screening of ISGs for antiviral activity against Dengue virus (DNV) and West Nile virus showed viperin, ISG20, PKR and IFITM2/3 as the major antiviral effectors [63]. In a study that characterized ISG profile by testing for 380 genes for antiviral activity against six pathogenic viruses, a group of ISGs showed broad antiviral activity while others showed more restricted specificity [117]. Specifically, IRF1, IFITM3, Rig-1, MDA5 were identified as broad acting antiviral effectors [116, 117]. When antiviral activity was analyzed for each virus, a unique ISG profile was observed for each virus with some overlap in the profile across different viruses. More importantly, studies have shown that antiviral activity for most ISGs studied falls in a spectrum in which a group of ISGs show low to moderate antiviral activity while others show very high antiviral activity [117]. Also, it has been shown that the antiviral activity is greater when pairs of ISGs were expressed as compared to either one alone, indicating that ISGs work together to reinforce the IFN induced antiviral activity [116].

1.3.3.3 Antagonism of the antiviral response and IFN signaling by viruses

Viruses have evolved countermeasures to subvert the antiviral defense mechanism of the host. Viruses encode for proteins that can impede antiviral response either at the level of interferon synthesis or at the JAK-STAT signaling [56, 69, 81]. One of the important groups of virus in this regard is the paramyxoviruses, a family of negative sense RNA viruses. Some of the viruses belonging to the paramyxovirus family typically undergo G-nucleotide insertion editing that leads to frameshift in transcription. The proteins that are important in the IFN antagonism are P protein and the V protein that are generated as a result of the frameshift [56]. These proteins inhibit IFN by targeting its components which include PRRs (Rig-1, MDA5), IRF3, and STAT1/2 [22, 56]. The NS1 protein of Influenza A virus, an orthomyxovirus, is known to target the Rig-1 receptors as these PRRs play an important role in the detection of Influenza virus RNA. The NS1 protein inhibits Rig-1 mediated antiviral signaling by blocking the ubiquitination of RIG-1 that is dependent on the activity of TRIM25 [44, 56]. The IFN regulatory factor, chiefly IRF3 is another target for the viral proteins [22]. Paramyxovirus V protein inhibits IRF3 by polyubiquitination and degradation of IKKε/TBK1, thereby preventing IRF3 phosphorylation and translocation into the nucleus [56]. Likewise, HPV-16 E6 proteins directly inhibit IRF3. On the other hand BGLF4 protein of Epstein-Barr virus (EBV) is known to decrease the active, phosphorylated IRF3 thereby reducing the IFN response [56, 139].

The type I and type III IFN JAK-STAT signaling converges at the level of STAT1/STAT2 heterodimer formation. The EBOV VP24 protein inhibits the nuclear translocation of the phosphorylated STAT1/STAT2 [154]. On the other hand, the V proteins of paramyxoviruses target the STAT1 and STAT2 for proteasomal degradation

that is dependent on the polyubiquitination of the STAT proteins [56]. The nuclear translocation of ISGF3 is inhibited by HPV-16 E7 proteins [7]. In addition, some paramyxoviruses inhibit IFN signaling by sequestering STAT1 and STAT2 within the cytoplasm [56]. The Sendai virus C protein inhibits phosphorylation of tyrosine and serine residues on the STAT1/STAT2 [56]. Therefore, degradation, dysregulation in phosphorylation, and sequestration of the STAT1/SAT2 are common strategies used by viruses to antagonize the IFN induced antiviral response.

1.4 A brief overview of Zinc metalloprotease-ZMPSTE24

ZMPSTE24 is a transmembrane zinc-metalloprotease whose catalytic activity is dependent on the highly conserved HEXXH motif [65, 106, 107]. ZMPSTE24 has promiscuous substrate specificity; it cleaves both prenylated and non-prenylated substrates [55]. It cleaves the three amino acids within the C-terminal CAAX motif, releasing the –AAX from the CAAX motif [9]. The ZMPSTE24 is an ortholog of the Ste24p in yeast, sharing high degree of sequence identity with Ste24p [8]. In yeast, the Ste24 is required for the maturation of the mating pheromone a-factor [94]. In mammals, ZMPSTE24 is critical for the processing of the prelamin A precursor to lamin A, a critical component of the nuclear lamina [9, 55, 122]. ZMPSTE24 is constitutively expressed and is localized in the inner nuclear membrane. Lamins are intermediate filament proteins that regulate the structure and shape of the nuclear envelope [49]. The processing of the precursor premlamin A to lamin A includes three steps: farnesylation of cysteine, removal of –AAX, and methylation of the farnesylcysteine. The mature lamin A is formed following removal of fifteen amino acids from the C-terminus [9, 122].

Mice defective in the ZMPSTE24 gene show accelerated ageing, resembling the Hutchinson-Gilford Progeria Syndrome (HGPS), or disease resulting from LMNA gene

(which encodes for prelamin A) mutation [20, 40]. In ZMPSTE24$^{-/-}$ mice, there is increased accumulation of the prelamin A, deficiency in mature lamin A, and defectively shaped nuclear envelope [40]. ZMPSTE24 deficient mice show bone fracture and muscle weakness [13].

1.4.1 ZMPSTE24 as a host restriction factor

Recently, ZMPSTE24 has been shown to restrict a number of enveloped viruses that depend on low pH for fusion [43]. ZMPSTE24 inhibits a diverse array of enveloped RNA viruses including IAV, Zika, Ebola, etc., as well as DNA viruses, chiefly cowpox and vaccinia virus [43]. However, murine leukemia virus (an RNA virus) and adenovirus (a DNA virus) were shown to be resistant to ZMPSTE24 [43]. In a recent study, ZMPSTE24 was shown to work in cooperation with IFITM3 to inhibit entry of arenaviruses [123]. In general, ZMPSTE24 restricts fusogenic viruses that depend on the low pH environment of the endosomes for fusion [43]. Since adenovirus is lysogenic, it is plausible that this group of viruses is resistant to ZMPSTE24 [43]. Like IFITM3, ZMPSTE24 is constitutively expressed. However, unlike IFITM3, ZMPSTE24 protein is not upregulated by interferon treatment [43]. ZMPSTE24 was identified as one of the binding partners of IFITM3 and its association with IFITM3 is enhanced by interferon treatment [43]. Mice with defective ZMPSTE24 gene were highly susceptible to IAV infection. However, interferon treatment, which upregulates IFITM3 expression thereby recruiting more ZMPSTE24, restores the antiviral activity of IFITM3 [43, 84]. ZMPSTE24 has been proposed to function as a downstream effector of IFITM3 [84, 123]. Studies suggest that ZMPSTE24 exerts its antiviral activity via its interaction with IFITM3, chiefly during entry of virus into the endosomes. In cells overexpressing ZMPSTE24, this restriction factor was shown to block IAV entry by trapping viruses

within the highly acidic endosomes [43]. Therefore, ZMPSTE24 restricts IAV by preventing cytosolic release. PRRSV is an enveloped RNA virus that depends on endosomal trafficking for cytosolic entry. Given the ability of ZMPSTE24 to restrict a wide variety of enveloped RNA viruses, studying the role of this restriction factor on PRRSV replication may reveal more on PRRSV and its interaction with host restriction factors.

Chapter 2: Interferon induced transmembrane protein 3 (IFITM3) restricts PRRSV replication via post-entry mechanisms

Pratik Katwal[1], Eric Nelson[2], Michael Hildreth[1], Shitao Li[3], Xiuqing Wang[1*]

[1]Department of Biology and Microbiology, South Dakota State University, Brookings, SD, 57007, USA

[2]Department of Veterinary and Biomedical Sciences, South Dakota State University, Brookings, SD, 57007, USA

[3]Department of Microbiology and Immunology, Tulane University, New Orleans, LA 70112, USA

*Corresponding author: Xiuqing.Wang@sdstate.edu

2.1 Abstract

Interferon induced transmembrane protein 3 (IFITM3) is a member of the family of interferon stimulated genes (ISGs) that inhibits a diverse array of enveloped viruses which enter into host cell by endocytosis. Porcine reproductive and respiratory syndrome virus (PRRSV) is an enveloped RNA virus causing significant economic losses to the swine industry. Very little is known as to how IFITM3 restricts PRRSV. In this study, the role of IFITM3 in PRRSV infection was studied *in vitro* using MARC-145 cells. IFITM3 overexpression reduced PRRSV replication, while siRNA induced knockdown of endogenous IFITM3 increased PRRSV RNA copies. Colocalization of virus with IFITM3 was observed at both 3 and 24 hours post infection (hpi). Amphotericin B only partially restored PRRSV replication in MARC-145 cells. Accordingly, very little co-localization between PRRSV and the late endosome and lysosome marker (LAMP-1) was observed. Quantitative analysis of confocal microscopic images showed that an average of 73% of IFITM3 expressing cells were stained positive for PRRSV at 3 hpi, while only an average of 27% of IFITM3 expressing cells were stained positive for PRRSV at 24 hpi. These findings suggest that IFITM3 may restrict PRRSV at the post-entry steps. Future studies are needed to better understand the mechanisms by which this restriction factor inhibits PRRSV.

Key words: virus restriction factors, interferon stimulated genes (ISGs), Interferon induced transmembrane protein 3 (IFITM3), porcine reproductive and respiratory syndrome virus (PRRSV)

2.2 Introduction

Restriction factors function to antagonize virus infection and can target viruses at various stages of their life cycle. They block cytosolic entry of enveloped viruses by either directly inhibiting virus fusion at the cell surface or by preventing fusion within the endosomes [115]. The Interferon induced transmembrane protein 3 (IFITM3) belongs to a class of interferon stimulated genes (ISGs) that inhibits viral-host membrane fusion within the endosomes [104]. Some of the well-studied classical ISGs include MX1, OAS, and PKR that play important role during virus infection [52, 99, 116]. IFITM proteins are constitutively expressed in various cell types and are potently induced upon interferon treatment [39, 42]. Of the five known members of the IFITM family, IFITM1, 2, and 3 are antiviral restriction factors and inhibit viruses that either enter by direct fusion with the cell membrane (IFITM1), or by endosomal trafficking (IFITM2 and IFITM3) [6, 16].

The role of IFITM3 in Influenza A virus (IAV) infection has been very well studied [4]. IFITM3 knockout mouse embryonic fibroblasts (MEFs) are highly susceptible to IAV infection [16]. The cytosolic release of the IAV viral ribonucleoproteins (vRNPs) is restricted by IFITM3, thereby blocking their subsequent nuclear entry [39, 104]. Enveloped viruses such as IAV that are pH sensitive and require low pH for fusion are highly restricted by IFITM3 [121]. The IFITM3 protein is expressed in the early or late endosomes and strongly inhibits viruses that enter through late endosomes. Overall, the block to virus uncoating results in the trapping of viruses in the acidic endolysosomes within which it undergoes degradation [39]. IFITM3 expression has been shown to expand acidified endosomes as evident from colocalization with endosomal markers, chiefly Rab7 and LAMP-1 [39]. Other viruses such as West Nile virus, vesicular stomatitis virus, etc. that fuse at pH greater than 6 are also inhibited

by IFITM3 [47, 142]. IFITM3 proteins inhibit a broad spectrum of enveloped RNA viruses [16, 47]. Recently, IFITM3 has also been shown to restrict Zika virus, an important emerging pathogen [112].

Porcine reproductive and respiratory syndrome virus (PRRSV) is an enveloped, positive sense, and single stranded RNA virus. It is a highly pathogenic virus that mainly causes respiratory disease in newborn pigs and reproductive disease in sows [32]. PRRSV belongs to the order *Nidovirales* within the family *Arteriviridae* [32]. Upon initial binding and internalization via binding to the sialoadhesin molecules, PRRSV enters into early endosome through a clathrin-dependent pathway in clathrin coated vesicles and is dependent on its binding to the CD163 receptor [96, 156]. CD163 functions as the principal PRRSV receptor that recycles between plasma membrane and endosomes [19, 144, 156]. PRRSV is known to enter into the endocytic pathway for cytosolic entry [73, 96]. However, one study showed that PRRSV does not appear to be associated with later endosome/lysosomes [131].

The impact of many ISGs including IFITM3 on PRRSV replication has not been extensively studied. One recent study has reported the antiviral role of IFITM3 on PRRSV infection [153]. Zhang et al. showed that IFITM3 did not block PRRSV entry into endosome or lysosome, but restricted PRRSV fusion through cholesterol accumulation within endosomal membrane [153]. These authors have further suggested that IFITM3 is incorporated into PRRSV virions, which results in reduced infectivity and cell-cell spread of PRRSV [38]. In this study, we have examined the role of IFITM3 in PRRSV replication in MARC-145 cells. Our data suggests that IFITM3 does not impact virus entry, but restricts PRRSV replication at post-entry steps.

2.3 Materials and methods

2.3.1 IFITM3 transfection in MARC-145 cells

MARC-145 cells were seeded at $2x10^5$ cells per well in a 12-well plate in DMEM medium supplemented with 10% FBS and 1% Penicillin-Streptomycin (complete DMEM medium). The 12-well plate was incubated in a humidified chamber at 37°C with 5% CO_2. After 24 h, cells were washed two times in DMEM medium and transfected with 1.25 μg of either the pQCXIP vector control (Q-series retroviral vector; Retro-X Q Vector Set) (Clontech, Cat. No. 631516; Takara Bio Inc.) or pQCXIP expressing the IFITM3-HA [16, 43] in triplicate wells using lipofectamine 3000 Transfection kit (Invitrogen), following the manufacturer's protocol. The retroviral vector pQCXIP carries puromycin resistant gene and expresses IFITM3-HA, transfected in HEK293 packaging cells for stable expression [43]. Transfection mix prepared as a 1:1 mixture of DNA and lipofectamine diluted in DMEM medium was added to each well. Briefly, each of the plasmid DNA was diluted in DMEM medium with P_{3000} and mixed with Lipofectamine 3000 reagent diluted in DMEM. The transfection mix was then incubated at room temperature (RT) for 20 min after which 200 μl of the DNA-lipid complex was added dropwise to the respective wells in DMEM medium. After incubation for 6 h at 37°C, the medium was replaced with complete DMEM growth medium. After 72 h, each of the six wells was infected with PRRSV 23983 at an MOI of 1 for 24 h at 37°C. Then, cells together with supernatant were harvested by scraping, and centrifuged at 13,000 rpm for 3 min. The supernatant and the pellets were stored separately in 1.5 ml microcentrifuge tubes at -80°C until used for further analysis.

For colocalization or cytotoxicity experiment, MARC-145 cells at $1x10^4$ cells per well were seeded in two 8-chamber slides (colocalization study) or a 96-well plate (cytotoxicity study) in complete DMEM medium and incubated at 37°C for 24 h. Cells in 8-chamber slides and 96-well plate were transfected with 0.3 µg of either pQCXIP vector control or IFITM3-HA using lipofectamine 3000 reagent.

For transfection in a 48-well plate, MARC-145 cells were cultured at a seeding density of $5x10^4$ cells per well. The experiment was performed in two groups. In first group, cells were transfected with 0.3 µg of either pQCXIP plasmid vector or pQCXIP IFITM3-HA in triplicates using lipofectamine 300 reagent as described previously. In the second group, same transfection scheme was followed and then marked as Amphotericin B treatment group.

2.3.2 siRNA induced knockdown of IFITM3 in MARC-145 cells

MARC-145 cells at a seeding density of $2x10^5$ cells per well were cultured in a 12-well plate. Following 24 h incubation at 37°C, cells were transfected with either negative control siRNA (Ambion, cat. no. AM4642) or IFITM3 siRNA (Life technologies, siRNA ID#s195035) at a final concentration of 30 nM per well using Lipofectamine RNAi max reagent (Invitrogen) according to the manufacturer's protocol. Transfection with either negative control siRNA or IFITM3 siRNA was performed in triplicate wells. Briefly, the siRNA was mixed with RNAi max reagent diluted in DMEM medium in 1:1 ratio. The mixture was incubated at RT for 5 min after which 125 µl of the siRNA complex was added dropwise to the respective wells of MARC-145 cells in DMEM medium. These wells were pre-washed two times with DMEM medium. Following washing, the 12-well plate was then incubated at 37°C for 6 h. Then the

DMEM medium was replaced with complete DMEM growth medium and incubated for 72 h. Next, the cells in each well of the 12-well plate were infected with PRRSV 23983 at an MOI of 1 for 24 h after which cells were scraped and harvested with supernatant. Following centrifugation at 13000 rpm, supernatant and cell pellets were separated out and stored at -80^{o}C in 1.5 ml microcentrifuge tubes.

For cytotoxicity experiment, 1.2 µl of either negative control siRNA or IFITM3 siRNA at a concentration of 30 nM was used for transfection in triplicate wells of a 96-well plate. Thus 25 µl of transfection mix was added dropwise to the respective wells with DMEM medium and incubated at 37^{o}C for 6 h after which media was replaced with complete DMEM growth medium and incubated at 37^{o}C for 72 h.

2.3.3 Western blot analysis

Cell pellets were resuspended with 60 µl cell lysis buffer (0.01M Tris-HCl pH 8, 0.14 M NaCl, 0.025% NaN_3, 1% Triton x-100) treated with Halt^{TM} protease and phosphatase inhibitor cocktail (Thermo Scientific, catalog# 78441) at 1:100 dilution. Each lysate sample thus obtained from overexpression of either the pQCXIP vector or the IFITM3-HA was vortexed for 15 s. The tubes were then incubated for 1 h at 4^{o}C, with vortexing every 15 min. Each tube was then spun at 13,000 rpm for 1 min after which the lysate was transferred to a new tube. Next, 40 µl of each sample was mixed with 40 µl (equal volume) of 2x western blot loading buffer treated with beta-mercaptoethanol at 1:50 dilution and 40 µl was loaded in each well. Two gels were loaded with the lysate samples from each tube. Before loading, each sample in 1.5 ml microcentrifuge tubes was incubated at 95^{o}C for 5 min and then vortexed for 15 s. Each gel was run at 150 V for 1.5 h and then transferred to nitrocellulose membrane run at 100 V for 1 h. Each nitrocellulose membrane was blocked by incubating with 10 ml of blocking buffer (5%

milk powder in 1x PBST) at room temperature (RT) for 1 h with shaking. Then the membranes were washed with 1x PBST three times for 5 min each with shaking at RT. Next, the membrane was incubated by shaking overnight at 4^{o}C with 10 ml of respective primary antibodies prepared in 5% milk blocking buffer. The following primary antibodies were used: anti-HA mouse monoclonal 1^{o} Ab against HA tagged IFITM3 (6E2) (Cell Signaling Technology, cat. no. 2367) at 1:1000 dilution, anti-PRRSV SR-30 1^{o} monoclonal Ab (provided by Dr. Eric Nelson) at 1:300 dilution, and mouse monoclonal anti-beta actin-Ab (Sigma-Aldrich, catalog# A2228) at 1:5000 dilution. Next day, the membrane was washed with 1x PBST three times for 5 min each with shaking at RT. The membrane was then incubated while shaking at RT in dark with Goat anti-Mouse IRDye® conjugated 2^{o} Ab (LI-COR, catalog# 926-32210) diluted to 1:5000 in 1x PBST. The membrane was washed in 1x PBST and observed using LI-COR Odyssey Infrared Imaging System. Quantification of the protein (band) intensity was performed using Image J [113]. Beta-actin house keeping gene was used to calculate relative fold change in PRRSV N protein expression in IFITM3 overexpressing cells as compared to vector control cells.

2.3.4 Interferon stimulation of IFITM3 gene in MARC-145 cells

To study the dose dependent response of IFN-alpha treatment on IFITM3 gene expression, a 12-well plate was seeded with 1x10^{5} MARC-145 cells per well and incubated for 24 h at 37^{o}C. After 24 h incubation, in duplicate wells, MARC-145 cells were treated with IFN-alpha at a concentration of either 50 U/ml, or 100 U/ml, or 500 U/ml. The respective IFN-alpha concentrations were prepared by diluting the stock at a concentration of 8x10^{5} U/ml (stock pre-diluted in 0.1 % BSA and 1x PBS and stored in aliquots of 10 µl at -80^{o}C) to the respective IFN-alpha working concentrations in DMEM

complete medium. Two wells were marked as control wells (IFN-alpha untreated) and were incubated with 1 ml of DMEM complete medium only. After 12 h incubation, the medium was removed and each well was infected with 1 MOI of PRRSV 23983 for 24 h at 37^{o}C. Following incubation, the cells from each well were harvested by scraping and then centrifuged in 1.5 ml microcentrifuge tubes. The cell pellets were stored at -80^{o}C for analysis of IFITM3 gene expression and PRRSV N RNA copies by RT-PCR.

2.3.5 Immunofluorescence assay and flow cytometry

After 72 h transfection, Amphotericin B at a concentration of 2.5 µg/ml was added to each of the six wells of a 48-well plate transfected with either vector control plasmid pQCXIP or IFITM3-HA in triplicates. Another set of six wells that were transfected similarly in the same plate were not treated with Amphotericin B. After incubating the plate at 37^{o}C for 1 h, the medium with Amphotericin B drug was removed. PRRSV 23983 was added at an MOI of 1 to all wells and the plate was incubated at 37^{o}C for 24 h. Cells were then fixed with 80% acetone for 20 min at RT, followed by air drying. Next, FITC conjugated anti-PRRSV Ab specific to N protein (SDOW-17) (provided by Dr. Eric Nelson) [98] at 1:80 dilution was added to each well and incubated at 37^{o}C for 1 h. Cells in each well were washed in 1x PBS and then observed under immunofluorescence microscope for fluorescence staining specific to PRRSV. After observing, cells in each well were scraped using a cell scraper in 500 µl PBS, then analyzed by flow cytometry, and mean fluorescence intensity for FITC staining was calculated. The images were captured at 10x magnification using an Olympus IX70 Inverted-Microscope (Epi-fluorescence and phase contrast).

2.3.6 Colocalization study using confocal microscopy

For the study of colocalization of PRRSV with endosomal markers, MARC-145 cells were seeded at $1x10^4$ cells per well in three 8-chamber slides for each time point study. After culturing for 24 h, the cells were infected with PRRSV at an MOI of 10. Then at three time points-1 h, 3 h, or 6 h after infection, the cells in respective slides were fixed with 3.8% formaldehyde for 10 min at RT, then washed in 1x PBS for 5 min and treated with 0.2% Triton x-100 for 10 min, after which cells were again washed once and incubated with 5% goat serum in PBS (blocking buffer) for 1 h. Then cells were stained with SDOW-17 (FITC conjugated anti-PRRSV N) monoclonal Ab at 1:80 dilution, together with either anti-EEA1 Ab (Santa Cruz Biotechnology, sc-365652) or anti-LAMP-1 Ab (Santa Cruz Biotechnology, sc-19992) conjugated to Alexa Fluor 647. Following incubation, the cells were washed three times with 1x PBS, then mounted using ProLong Gold antifade mounting reagent (Invitrogen). Then the slides were observed by confocal microscopy. For the quantification of colocalization, Image J was used [113, 114]. Briefly, for each time point, five random cells were selected and then with manual thresholding, the threshold range was selected to define the object of interest distinct from the background (Image J) [114]. The color (yellow) threshold was adjusted to measure the area of colocalized region (A1). Next, the threshold color was adjusted to select all five cells to obtain area of the total five cells (A2). The percentage colocalization was calculated by multiplying the fraction, (A1/A2) by 100. Mean percent colocalization was calculated for each time point from three selected areas (each with five cells).

MARC-145 cells cultured in two 8-chamber slides were transfected with either vector control pQCXIP or IFITM3-HA in duplicate wells of each slide as described

earlier. For 3 hours post infection (3 hpi) study, PRRSV 23983 at an MOI of 4 was added to all wells except one vector control transfected well. For 24 hpi study, cells were infected with PRRSV at an MOI of 1. After infecting cells with PRRSV for the respective times, the two slides were fixed in 3.8% formaldehyde for 10 min at RT followed by one wash in 1x PBS for 5 min. The cells in each well were then treated with 0.2% Triton x-100 diluted in 1x PBS for permeabilization and incubated at RT for 10 min. Next, the cells were washed and incubated at RT for 30 min with 5% goat serum in PBS for blocking non-specific antibody binding. After washing in 1x PBS, cells in each well were incubated overnight at RT with primary antibody diluted in 5% goat serum. Mouse monoclonal anti-HA primary antibody against HA tagged IFITM3 (6E2) (Cell Signaling Technology, cat. no. 2367) was added at a dilution of 1:1600 to all wells except the uninfected vector control transfected well to which 5% goat serum was added. Next day, the slides were washed three times with 1x PBS for 5 min each and then incubated for 1 h at 37^{o}C with secondary antibody. To the three wells incubated with anti-Flag primary antibody, Alexa fluor 647 conjugated goat anti-mouse IgG 2^{o} Ab (Abcam) at 1:200 dilution was added. After 1 h incubation, cells were washed and incubated with 1:80 diluted anti-PRRSV FITC conjugated Ab (SDOW17) at 37^{o}C for 1 h. The uninfected vector control transfected well was incubated with Alexa fluor 647 2^{o} Ab only. The two slides were washed, counterstained with DAPI, and then mounted as described previously. The slides were then stored at 4^{o}C overnight and then observed using Olympus Fluoview FV1200 Laser Scanning Confocal Microscope to study colocalization of PRRSV and IFITM3 at 3 or 24 hpi. Briefly, five different microscopic fields at 40x magnification were analyzed by confocal microscopy for each of the pQCXIP vector

control transfected group and IFITM3-HA transfected group. In each field, cells were counted by DAPI staining and then the percentage of cells staining for PRRSV (green) or IFITM3 (red) was calculated. Colocalization study was performed by counting the number of DAPI stained cells with yellow fluorescence which is observed due to overlap of the emission spectra for green (FITC conjugated Ab for PRRSV N at 488 wavelength) provided by Dr. Eric Nelson [98] and red (Alexa fluor 647 conjugated Ab for IFITM3) (Abcam) dyes. Uninfected control cells stained with FITC conjugated anti-PRRSV Ab were used as a control for comparing the background (green) staining with the PRRSV infected group.

2.3.7 Cytotoxicity assay

MARC-145 cells cultured in a 96-well plate were transfected with either the pQCXIP vector control or pQCXIP expressing IFITM3-HA or negative control siRNA (Ambion, cat. no. AM4642) or IFITM3 siRNA (Life technologies, siRNA ID# s195035) in triplicate wells, as described earlier. After 72 h, each well of the 96-well plate incubated with 200 µl of DMEM growth medium was treated with 10 µl of CCK-8 solution (Sigma, cat. no. 96992) and incubated at 37^{o}C for 3 h, after which absorbance was measured at 450 nm using a Synergy 2 plate reader (BioTek).

2.3.8 Real-time reverse transcription PCR (RT-PCR)

Total RNA extraction was done from cells harvested earlier using RNeasy Mini Kit (Qiagen Cat. No. 74104), following the manufacturer's protocol. To generate cDNA, 1 µg of the total RNA extracted was reversed transcribed using High Capacity cDNA Reverse Transcription Kit (applied biosystems) under following reaction conditions: 25^{o}C for 10 min, 37^{o}C for 120 min, and 85^{o}C for 5 min (Applied Biosystems GeneAmp PCR System 2400). Real time PCR was performed by using 3 µl of the cDNA

product as template for each reaction using Brilliant II SYBR Green QPCR master mix (Agilent Technologies). Forty cycles of following conditions were used: 95°C for 10 min, 95°C for 30 s, 55°C for 30 s, and 72°C for 30 s. Primers specific to beta-actin housekeeping gene, PRRSV N, IFITM3, and Mx1 are shown in Table 2.1. The reactions were run in a QuantStudio 6 Flex *Real-Time PCR* System (Applied Biosystems). Data analysis was performed by calculating the mean fold change in gene expression using the ΔΔCT method. Housekeeping gene beta-actin was used as a reference gene for comparing the fold change between two treatment groups [88].

2.3.9 $TCID_{50}$ titer

Fifty-percent tissue culture infectious dose ($TCID_{50}$) assay was performed to determine the infectious PRRSV 23983 titer in the supernatant at 24 hpi obtained from the previously described IFITM3 overexpression or siRNA induced knockdown experiments. $TCID_{50}$ titer was determined using the Spearman-Karber method [79].

2.3.10 Statistical analysis

A two tailed student's t-test was used to compare the PRRSV titer between pQCXIP vector control and IFITM3-HA transfected group. Likewise, relative fold change in IFITM3 or PRRSV N mRNA gene expression was compared. Using t-test, the mean fluorescent intensity was compared between vector control and IFITM3 overexpressing MARC-145 cells in both Amphotericin B treated and untreated group. In all the statistical analysis, a p value less than 0.05 ($p<0.05$) was considered as significant.

Table 2.1 Primer sequences of IFITM3, PRRSV N, and the house-keeping gene (beta-actin).

Gene	**Forward Primer (5'-3')**	**Reverse Primer (5'-3')**
beta-actin	TTGCTGACAGGATGCAGAAGGAGA	ACTCCTGCTTGCTGATCCACATCT
IFITM3	GGTCTTCGCTGGACACCAT	TGTCCCTAGACTTCACGGAGTA
PRRSV N	GTCAATCCAGACCGCCTTTA	GATCAGGCGCACAGTATGAT
Mx1	TTTTCAAGAAGGAGGCCAGCAA	TCAGGAACTTCCGCTTGTCG

2.4 Results

2.4.1 Over-expression of IFITM3 reduces PRRSV replication

Western blotting analysis confirmed the expression of exogenous IFITM3 in cells transfected with plasmid containing IFITM3-HA (Fig. 2.1 A), but not in cells transfected with pQCXIP vector control (Fig. 2.1A). A slightly reduced expression of PRRSV N protein was observed in cells expressing exogenous IFITM3 (Fig. 2.1A). Quantification of the protein band intensity showed an average of 31% reduction in PRRSV N protein expression in IFITM3 overexpressing cells as compared to vector control (Fig. 2.1B). Virus titers in the supernatants of cells harvested at 24 hpi showed an average of 5.4-fold decrease in IFITM3-HA transfected cells compared to vector controls (Fig. 2.1C). Cytotoxicity assay showed that there were no significant differences in cell viability

between vector control group and IFITM3 overexpressing group (Fig. 2.1D). The mean absorbance values of vector control group and IFITM3 overexpressing group were 1.48 and 1.32 respectively (Fig. 2.1D). Taken together, these results suggest that overexpression of IFITM3 protein reduces PRRSV replication.

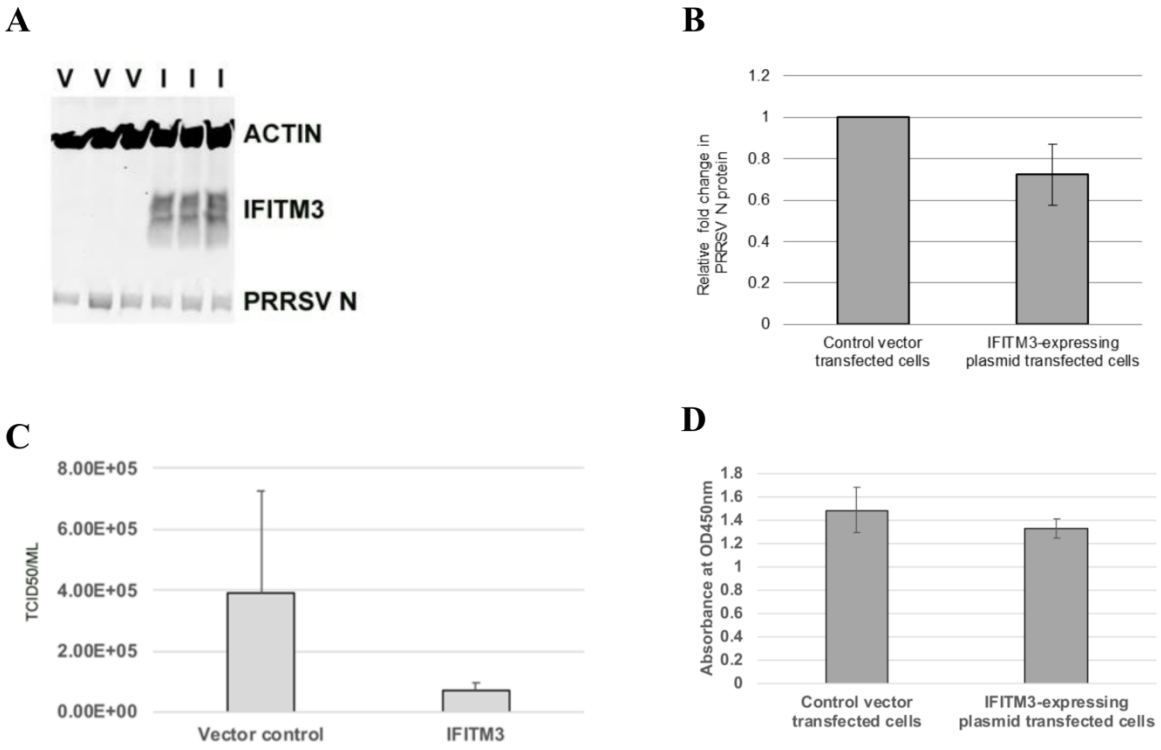

Fig. 2.1 Over-expression of IFITM3 reduces PRRSV replication. **A:** Representative western blotting analysis showing the expression of exogenous IFITM3 in cells transfected with plasmid containing IFITM3 (I), but not in cells transfected with vector control (V). **B:** Quantitative analysis of the band intensity from western blot assay using Image J. About 31% reduction in expression of PRRSV N protein is also observed in cells expressing exogenous IFITM3 compared to vector control. **C:** Virus titers in the supernatants of cells transfected with vector control or IFITM3 containing plasmid at 24 h after virus infection. An average of 5.4-fold decrease was observed in IFITM3 transfected cells compared to vector controls. **D:** CCK-8 cytotoxicity assay was used to compare the difference in cell viability between pQCXIP vector control and IFITM3-HA overexpressing MARC-145 cells at 450 nm. A p value < 0.05 was considered as statistically significant.

2.4.2 Knockdown of IFITM3 by siRNA enhances PRRSV replication

To validate the knockdown of endogenous IFITM3, qRT-PCR was performed to analyze the fold change in gene expression in IFITM3 silenced MARC-145 cells as compared to control silencing RNA. qRT-PCR confirmed the silencing of IFITM3, with an average of 50% knockdown efficiency (Fig. 2.2A). Furthermore, qRT-PCR was performed to quantify the viral RNA copies in control silencing and IFITM3 silencing RNA transfected cells. An average of 1.28-fold increase in viral RNA copies was observed in IFITM3 silencing RNA transfected cells compared to control silencing RNA transfected cells (Fig. 2.2B). There were no significant differences ($p>0.05$) in cell viability between control silencing RNA and IFITM3 silencing RNA (Fig. 2.2C). The mean absorbance values of negative control silencing group and IFITM3 silencing group were 1.76 and 1.47 respectively (Fig. 2.2C). This shows that cytotoxicity does not play a

role in IFITM3 mediated PRRSV restriction. Overall, knockdown of IFITM3 slightly affected virus replication.

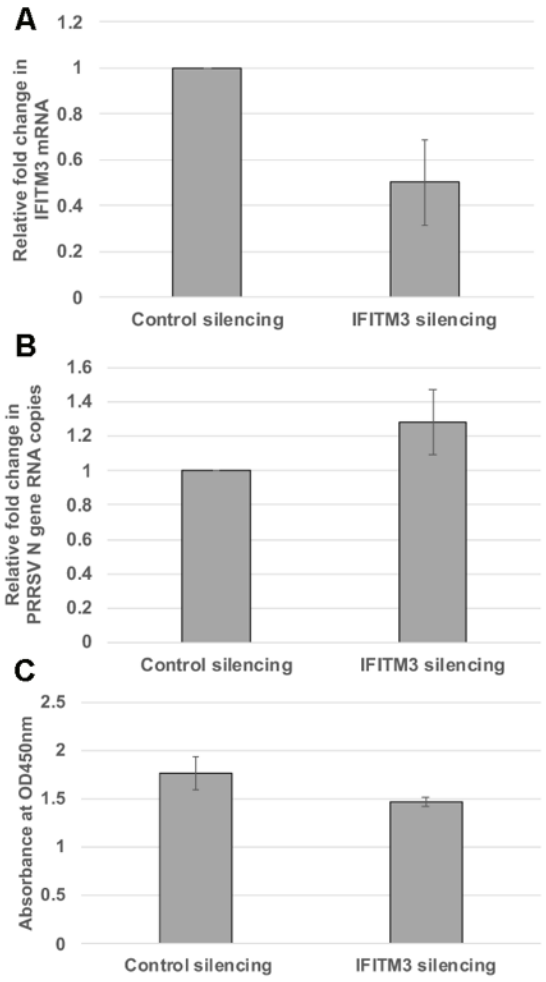

Fig. 2.2 Knockdown of IFITM3 by siRNA enhances PRRSV replication. **A:** qRT-PCR showing the silencing of IFITM3. **B:** qRT-PCR showing the viral RNA copies in control silencing and IFITM3 silencing RNA transfected cells. An average of 1.28-fold increase in viral RNA copies was observed in IFITM3 silencing RNA transfected cells compared to control silencing RNA transfected cells. **C:** Difference in cell viability was compared between the negative control siRNA and IFITM3 siRNA transfected MARC-145 cells. Graph shows mean absorbance values read at 450 nm between the two groups. A p value < 0.05 was considered as significant.

2.4.3 Positive correlation between interferon-induced IFITM3 upregulation and reduced PRRSV replication

When compared to non-treated control group, PRRSV infection in MARC-145 cells upregulated the Mx1 gene expression but not IFITM3 (Fig. 2.3A). IFN-alpha treatment induced mRNA gene expression of both IFITM3 and Mx1 as compared to the control group (Fig. 2.3A). At 50 U/ml IFN-alpha concentration, the mean fold change in IFITM3 gene expression as compared to IFN-alpha untreated cells was 1.94 (Fig. 2.3B). At 100 U/ml concentration of IFN-alpha, the mean fold change in IFITM3 gene expression was 3.73 (Fig. 2.3B). At 500 U/ml concentration of IFN-alpha, the mean fold change in IFITM3 expression was 4.91 (Fig. 2.3B). As compared to the IFN-alpha untreated group infected with PRRSV, the mean fold change in PRRSV N gene transcripts upon treatment with IFN alpha at 50 U/ml, 100 U/ml, and 500 U/ml were 0.34, 0.16, and 0.07 respectively (Fig. 2.3B). These results demonstrate the dose dependent response of IFITM3 upon IFN-alpha treatment and PRRSV replication in MARC-145 cells is inversely correlated to the IFITM3 expression.

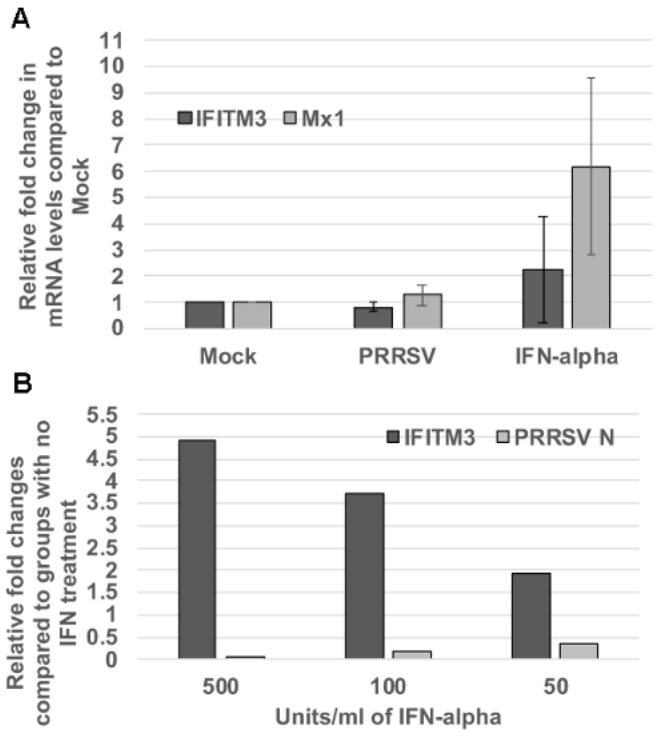

Fig. 2.3 Positive correlation between interferon-induced IFITM3 upregulation and reduced PRRSV replication. **A:** Relative fold changes in IFITM3 and Mx1 gene expression in PRRSV 23983 infected groups when compared to mock treated groups are shown. More abundant Mx1 as compared to IFITM3 mRNA is induced by IFN-alpha. **B:** Real-time RT-PCR shows the relative fold changes of IFITM3 and PRRSV N mRNA gene expression in IFN-alpha treated groups at different concentrations when compared to non-treated control groups.

2.4.4 Amphotericin B treatment only partially restores PRRSV replication in IFITM3 overexpressing MARC-145 cells

Immunofluorescence staining showed that IFITM3 overexpression significantly reduced PRRSV infection in MARC-145 cells (Fig. 2.4A). To quantitatively estimate the

PRRSV infection in the Amphotericin B treated and untreated group, flow cytometry was performed. Analysis of virus-infected cells in the presence or absence of Amphotericin B treatment confirmed that Amphotericin B only partially restored the replication of PRRSV in cells over-expressing IFITM3 (Fig. 2.4B). In the Amphotericin B untreated group, a significant reduction in mean fluorescence intensity ($p < 0.05$) in the IFITM3 overexpressing cells as compared to vector control was observed (Fig. 2.4B). This data further validates our observation shown in Fig. 2.1

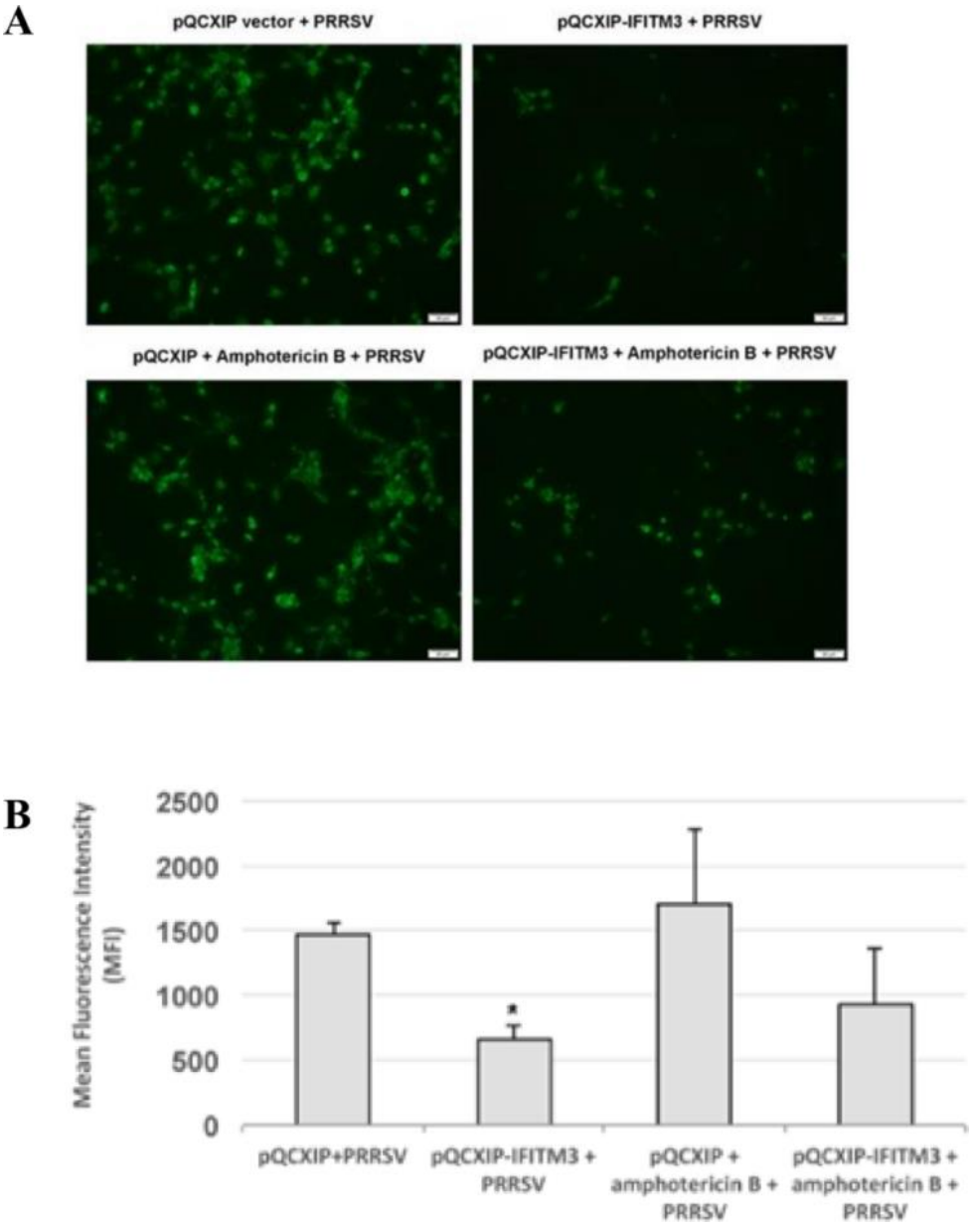

Fig. 2.4 Amphotericin B treatment only partially restores PRRSV replication in IFITM3 overexpressing MARC-145 cells. **A:** Immunofluorescence staining of virus-infected cells in the presence or absence of Amphotericin B treatment. Images were captured at 10x magnification. **B:** flow cytometry analysis of virus-infected cells in the presence or absence of Amphotericin B. * indicates $p < 0.05$ when compared to the pQCXIP + PRRSV group.

2.4.5 Colocalization of PRRSV with early endosome marker EEA1 at 3 hpi

To examine whether PPRSV enters the late endosomes during virus entry, MARC-145 cells infected with PRRSV 23983 for 1 h, 3 h, or 6 h were stained for either the early endosomal marker, EEA1 (Fig. 2.5A) or late endosome/lysosome marker, LAMP-1 (Fig. 2.5C). The mean percent colocalization between PRRSV and EEA1 was 23.8%, 37.9%, and 31.8% at 1 hpi, 3 hpi, and 6 hpi respectively (Fig. 2.5B). However, the mean percent colocalization with LAMP-1 was 5.7%, 11.6%, and 8% at 1 hpi, 3 hpi, and 6 hpi respectively (Fig. 2.5D). At each time point, a greater percentage of colocalization was observed between PRRSV and EEA1 than LAMP-1 (Fig. 2.5B, D). Stronger colocalization between PRRSV and EEA1 was observed at 3 hpi (Fig. 2.5B). A smaller percentage of colocalization between PRRSV and LAMP-1 was observed at 1 and 6 hpi as compared to 3 hpi (Fig 2.5D).

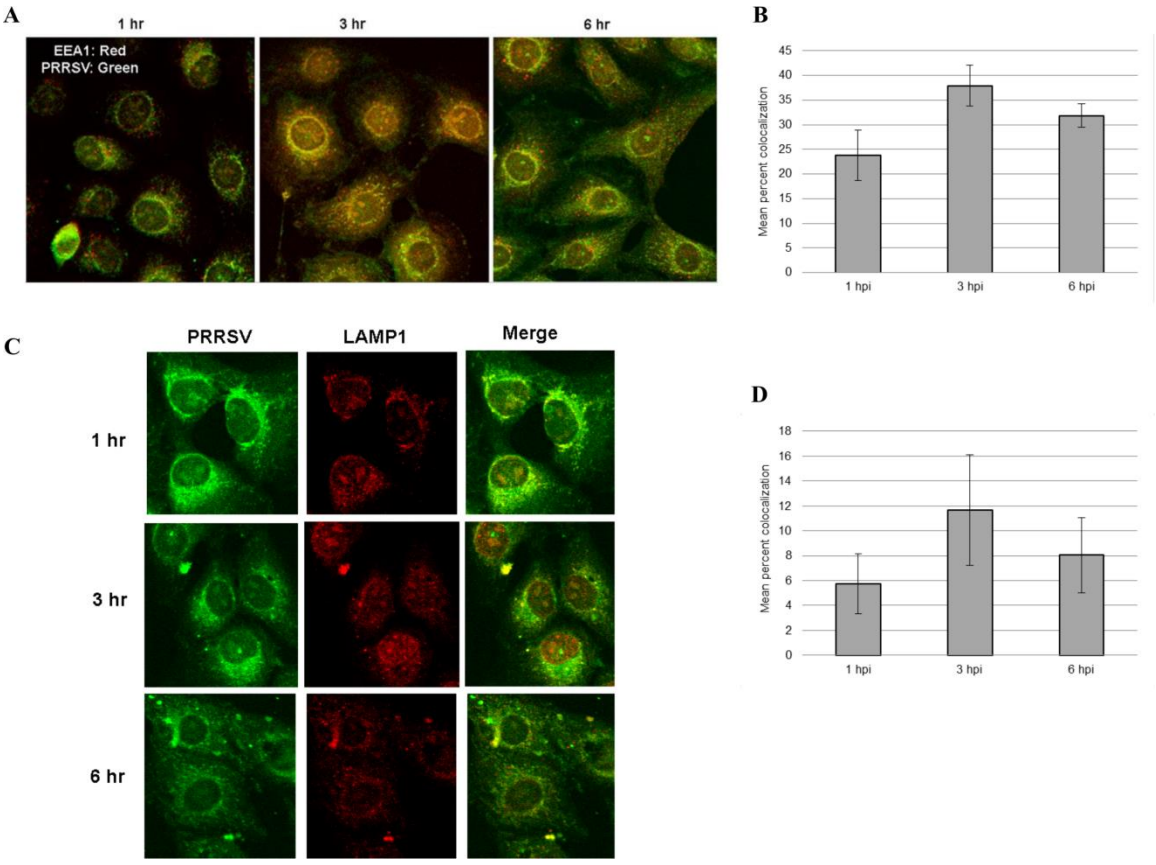

Fig. 2.5 Colocalization of PRRSV with early endosome marker EEA1 at 3 hpi. **A:** Colocalization of PRRSV with EEA1 at different time points. Tunneling nanotube-like filamentous extensions were observed at 3 h after virus infection. **B:** Mean percent colocalization was estimated using Image J. For each time point, mean percent colocalization was calculated by randomly selecting five cells for each microscopic field. Greater percentage of colocalization occurred with EEA1 at 3 hpi as compared to 1 or 6 hpi. **C:** Colocalization of PRRSV with LAMP-1 at different time points. **D:** Relatively fewer colocalization between PRRSV and late endosome/lysosome marker LAMP-1 was observed at 1 and 6 hpi as compared to 3 hpi. Images were captured using a confocal microscope at 40x magnification.

2.4.6 Over-expression of IFITM3 does not significantly impact virus entry

Cells over-expressing exogenous IFITM3 were stained for PRRSV at 3 and 24 hpi. Colocalization of IFITM3 with PRRSV was observed at both time points (Fig. 2.6A). An average 73% of IFITM3 expressing cells contained virus at 3 hpi, while only approximately 27% of IFITM3 expressing cells contained virus at 24 hpi (Fig. 2.6B). Confocal images of control vector transfected cells showed clusters of virus-infected cells at 24 hpi (data not shown), indicative of efficient cell-cell spread of virus. In contrast, IFITM3 over-expressing cells typically showed a few punctuate positive virus staining within isolated individual cells at 24 hpi (Fig. 2.6A).

A

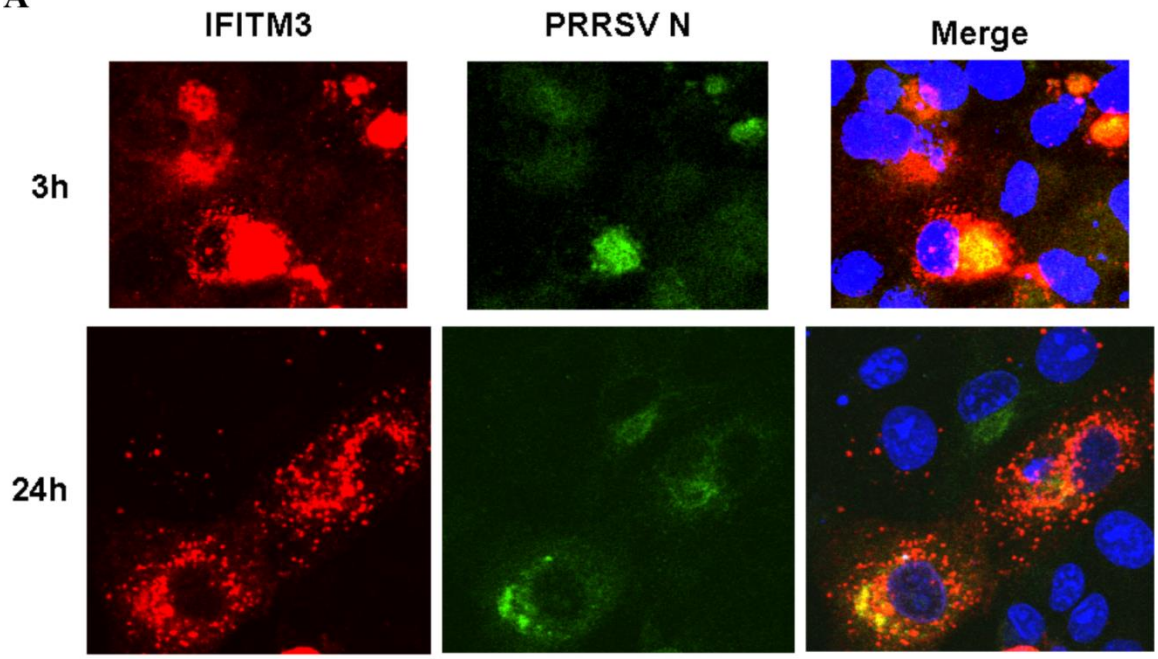
IFITM3
PRRSV N
Merge
3h
24h

B

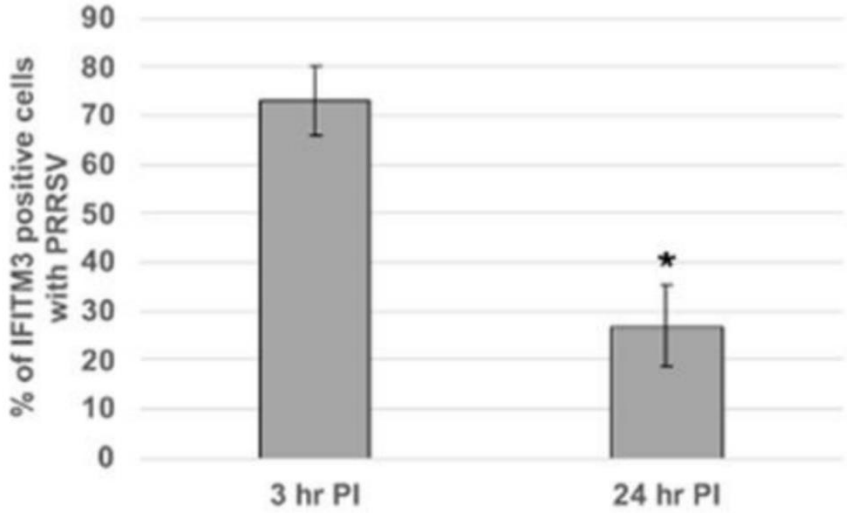
% of IFITM3 positive cells with PRRSV
90
80
70
60
50
40
30
20
10
0
*
3 hr PI
24 hr PI

Fig. 2.6 Over-expression of IFITM3 does not significantly impact virus entry. **A:** Cells over-expressing exogenous IFITM3 contains PRRSV at 3 and 24 hpi. Red: IFITM3; Green: PRRSV N; Blue: DAPI. The colocalization of PRRSV with over-expressed IFITM3 is shown. Images were taken at 40x magnification. **B:** The percentage of PRRSV positive cells was significantly lower ($p < 0.0001$) in IFITM3 transfected cells at 24 hpi than that of 3 hpi. Quantification was done by counting PRRSV positive cells and IFITM3-HA expressing cells obtained from five different microscopic fields.

2.5 Discussion

IFITM3 is an interferon induced antiviral gene and partly contributes to the antiviral effect of interferon. Indeed, IFITM3 has been shown to restrict the replication of a diverse array of enveloped RNA viruses including PRRSV [39, 41, 112]. We have shown here that over-expression of IFITM3 reduced PRRSV replication in MARC-145 cells, which is consistent with the previous observation made by others [153]. Similarly, silencing of IFITM3 enhanced PRRSV replication as shown by both our study and Zhang, et al. [153]. The observed virus replication enhancement effect in our study is lower than what has been described in a previous study [153], which could be due to the relatively low knockdown efficiency (an average of 50%) in our study. Collectively, both overexpression and RNA silencing of IFITM3 data suggest its antiviral effect against PRRSV.

IFITM3 is constitutively expressed in both MARC-145 cells and porcine alveolar macrophages (PAMs). Our study and others [153] have shown the upregulation of IFITM3 protein upon IFN-α treatment, which is positively correlated with reduced PRRSV replication. PRRSV was shown to up-regulate IFITM3 gene expression in PAMs at 24 hpi [153]. Interestingly, we observed that PRRSV infection reduced IFITM3 gene

expression in MARC-145 cells at 24 hpi. This discrepancy in results could be due to the different cell types used in each study.

It is generally believed that IFITM3 decreases membrane fluidity thereby inhibiting virus-host cell membrane fusion and cytosolic release [104]. Studies using single virus fusion assay have shown that IFITM3 restricts virus membrane fusion [31, 91]. One earlier study reported that PRRSV is associated with early endosome only and not late endosomes [131]. We found that PRRSV colocalized with the early endosome marker EEA1 at 3 hpi, but most disappeared from early endosome at 6 hpi. Relatively fewer PRRSV colocalized with LAMP-1, a marker of late endosome and lysosome, during the first 6 hpi. IFITM3 is known to restrict virus membrane fusion and trap virus in late endosome for degradation [3, 138]. Amphotericin B treatment has been shown to fully restore infection of many viruses that are restricted by IFITM3 [86, 91]. In a recent study, Amphotericin B reversed the IFITM3 mediated entry-restriction of several pseudovirus particles tested, including SARS-CoVpp and IAVpp, but not LASVpp [158]. Amphotericin B is an antifungal drug known to restore membrane fluidity thereby reversing the effect of IFITM3 mediated virus restriction [86]. It forms leak ion channels in the cell membrane and has also been shown to associate with cholesterol in lipid rafts [138]. Our observation suggests that IFITM3 may restrict PRRSV in a mechanism different from SARS-COV and IAV [158] since fewer viruses were detected in late endosome. This observation is also consistent with our data showing that Amphotericin B treatment only partially restores PRRSV replication. Recently, Zhang et al. has shown that PRRSV colocalizes not only with early endosomes but also late endosomes/lysosomes at different stages of virus trafficking [153]. The discrepancy in

results could be due to different experimental conditions used in each study. Zhang et al. has also shown that IFITM3 does not restrict PRRSV attachment, entry, and internalization into endosomes, but inhibits virus membrane fusion via cholesterol induction in cellular vesicles [153].

Suddala et al. showed that IFITM3 expressing cells are not infected by IAV at 12 hpi, but adjacent cells not expressing IFITM3 are infected, suggesting that this antiviral activity of IFITM3 is not due to conditioned medium [124]. Our results showed that IFITM3 expressing cells do contain PRRSV at both 3 and 24 hpi, suggesting that a potential different mechanism mediates the antiviral activity to PRRSV than IAV. Suddala et al. suggests that IFITM3 accumulation at the sites of virus fusion prevents virus release into cytoplasm and replication [124]. We observed an average 73% of IFITM3 expressing cell contained PRRSV at 3 hpi, indicating that over-expression of IFITM3 has little effect on virus entry. However, at 24 hpi, only 27% of IFITM3 expressing cells contained PRRSV. Colocalization study showed that PRRSV in IFITM3 overexpressing MARC-145 cells exhibited a punctuated staining pattern in isolated individual cells at 24 hpi, while vector control cells typically showed clusters of virus positive cells (data not shown and Fig. 2.6A). These observations suggest that efficient cell-cell spread of virus may be affected by over-expression of IFITM3, which has also been shown by Zhang et al. [153]. Earlier studies have shown that PRRSV upregulates the formation of tunneling nanotubes (TNTs) to facilitate the intercellular spread of PRRSV [50]. Hence it is tempting to speculate that IFITM3 over-expression may affect cellular spread of virus by limiting formation of TNTs. Further studies are needed to uncover the impact of IFITM3 overexpression on formation of TNT upon PRRSV

infection. Overall, our data support a role of IFITM3 in restricting PRRSV post-entry into cells.

In conclusion, over-expression of IFITM3 reduced PRRSV infection in MARC-145 cells and may restrict PRRSV at the post-entry step since Amphotericin B treatment did not completely rescue PRRSV infection. Silencing of endogenous IFITM3 increased PRRSV-N RNA copies. Furthermore, a positive correlation between reduced PRRSV replication and interferon induced upregulation of IFITM3 was observed. Further study is needed to better understand the mechanisms by which IFITM3 restricts PRRSV replication in MARC-145 cells and porcine alveolar macrophages.

Acknowledgments

This study was partly supported by Agriculture and Food Research Initiative Competitive Grant no. 2021-67016-34460 from the USDA National Institute of Food and Agriculture, USDA NIFA Hatch (grant #1000514), Hatch Multi State (Grant #1010908), and South Dakota Agricultural Experiment Station.

Author Contributions

XW designed the study, analyzed data, and wrote the manuscript. PK (graduate student) conducted experiments, analyzed data and wrote the manuscript. EN and SL provided reagents/analytic tools. MH contributed to confocal microscopy and analysis.

Conflicts of Interest

The authors declare no conflict of interest.

Chapter 3: Role of Zinc Metalloprotease (ZMPSTE24) on Porcine Reproductive and Respiratory Syndrome Virus (PRRSV) Replication *In Vitro*

Pratik Katwal[1], Eric Nelson[2], Michael Hildreth[1], Shitao Li[3], Xiuqing Wang[1]*

[1]*Department of Biology and Microbiology, South Dakota State University, Brookings, SD, 57007, USA*

[2]*Department of Veterinary and Biomedical Sciences, South Dakota State University, Brookings, SD, 57007, USA*

[3]*Department of Microbiology and Immunology, Tulane University, New Orleans, LA 70112, USA*

*Correspondence: Xiuqing.Wang@sdstate.edu

3.1 Abstract

The transmembrane zinc metalloprotease, ZMPSTE24, works in cooperation with interferon induced transmembrane protein 3 (IFITM3) to restrict entry of several enveloped viruses. We investigated the role of ZMPSTE24 in porcine reproductive and respiratory syndrome virus (PRRSV) replication. ZMPSTE24 overexpression significantly reduced PRRSV replication in MARC-145 cells. Interestingly, knockdown of endogenous ZMPSTE24 did not significantly impact virus replication. There was no significant difference in the percentage of PRRSV positive cells and viral RNA copies at 3 hours post infection (hpi) between cells transfected with ZMPSTE24-FLAG and vector control. Our results suggest that ZMPSTE24 overexpression may restrict PRRSV replication at a post-entry step.

Key words: virus restriction factors, ZMPSTE24, Porcine Reproductive and Respiratory Syndrome Virus (PRRSV)

3.2 Introduction

Restriction factors such as interferon stimulated genes (ISGs) inhibit viruses at various stages of their life cycle [115]. Many enveloped viruses enter host cells by receptor mediated endocytosis. Triggered by acidic pH within endosomes, the viral fusion peptide undergoes conformational change and facilitates virus fusion with endosome membrane and uncoating. Several pH sensitive viruses that depend on low pH for fusion have been shown to be strongly inhibited by IFITM3 [121]. IFITM3 is localized in the early or late endosomes and impedes virus-host membrane fusion, thereby blocking release of the genome [6, 39]. The restriction factor ZMPSTE24 works in cooperation with the IFITM3 protein to restrict entry of several enveloped viruses [43, 84, 123]. ZMPSTE24 acts as a downstream effector of IFITM3 [43, 84]. The ZMPSTE24 protein is constitutively expressed and localized to inner nuclear membrane [8]. It is important in the processing of precursor prelamin A into lamin A in the nuclear lamina [8]. Defect in ZMPSTE24 has been shown to enhance accumulation of prelamin A [40]. Currently, there are very limited studies exploring the mechanism by which it restricts virus entry including its interaction with the IFITM proteins and IFITM independent virus restriction.

PRRSV is an enveloped, positive sense, single stranded RNA virus belonging to the family *Arteriviridae* within the order *Nidovirales* [90]. PRRSV causes severe respiratory disease in young pigs and reproductive failure in sows [90]. Upon attachment and internalization, PRRSV enters into the early endosome in clathrin-coated vesicles and virus-endosome membrane fusion leads to virus uncoating [131, 156]. The role of IFITM3 in restricting PRRSV replication has been recently reported [153]. However, very little is known whether ZMPSTE24 also restricts PRRSV replication. In this present

study, we investigated the role of ZMPSTE24 in PRRSV replication and examined whether ZMPSTE24 restricts PRRSV entry into cells.

3.3 Materials and methods

3.3.1 Plasmid transfection

A 12-well plate was seeded with $2x10^5$ cells per well of MARC-145 cells. The plate was incubated at 37°C in a humidified chamber with 5% CO_2 for 24 h. After 24 h incubation, the cells were washed with raw DMEM medium. In triplicate wells, cells were transfected with 1.25 µg per well of either pCMV-3Tag-8 control vector or FLAG-tagged ZMPSTE24 cloned into pCMV-3Tag-8 (ZMPSTE24-FLAG) plasmid [43] using Lipofectamine 3000 Transfection Kit (Invitrogen) according to the manufacturer's protocol. The plasmids were kindly provided by Dr. Shitao Li. Briefly, each of the plasmid DNA was diluted in raw DMEM medium with P_{3000} and mixed with Lipofectamine 3000 reagent diluted in raw DMEM in 1:1 ratio. The transfection mix was then incubated at room temperature for 20 min after which 200 µl of the DNA-lipid complex was added dropwise to the respective wells. For transfection in a 24-well plate, $5x10^4$ cells were seeded in each well and after 24 h incubation, transfected with 0.6 µg of each of the plasmids following similar protocol. The plates were incubated at 37°C for 6 h, then raw medium was removed and complete medium (DMEM with 10% FBS and 1% penicillin-streptomycin) was added. The plate was incubated at 37°C for 72 h and then PRRSV 23983 was added to each well at an MOI of 1. Following incubation at 37°C for 24 h, the cells were scraped and supernatant with cells was collected in 1.5 ml tubes. Each tube was centrifuged at 13,000 rpm for 3 min. The supernatant was collected and used in $TCID_{50}$ assay while cell pellets were stored for western blotting. For colocalization or cytotoxicity study, 0.3 µg of the respective plasmid DNA was used to

transfect MARC-145 cells that were seeded at $1X10^4$ cells per well in either the 8-chamber slide (colocalization study) or 96-well plate (cytotoxicity assay) and then incubated at 37°C for 72 h.

3.3.2 Silencing RNA (siRNA)

For siRNA induced knockdown study, MARC-145 cells cultured in a 12-well plate were transfected with either negative control siRNA (Ambion, cat. no. AM4642) or ZMPSTE24 siRNA (Life technologies, siRNA ID# s20067) at a final concentration of 30 nM per well in complete medium using Lipofectamine RNAi max reagent (Invitrogen) according to the manufacturer's protocol. Transfection with either negative control siRNA or ZMPSTE24 siRNA was performed in triplicate wells. Briefly, the siRNA was mixed with RNAi max reagent diluted in raw DMEM medium in 1:1 ratio. The mixture was incubated at RT for 5 min after which 125 µl of the siRNA complex was added dropwise to the respective wells with raw DMEM medium and then incubated at 37°C for 6 h. Then the raw medium was replaced with complete DMEM medium and incubated for 72 h. Next, the cells in each well of the 12-well plate were infected with PRRSV 23983 at an MOI of 1 for 24 h after which cells were scraped and harvested with supernatant and stored at -80°C until used for further study. For cytotoxicity experiment, 1.2 µl of either negative control siRNA or ZMPSTE24 siRNA at 30 nM concentration was used for transfection. In a 96-well plate, 25 µl of transfection mix was added dropwise to the respective wells with raw DMEM medium and incubated at 37°C for 6 h after which media was replaced with complete DMEM medium and incubated at 37°C for 72 h.

3.3.3 Western blotting

Cell pellets were resuspended with 60 µl cell lysis buffer (0.01M Tris-HCl pH 8, 0.14 M NaCl, 0.025% NaN_3, 1% Triton x-100) treated with Halt^{TM} protease and phosphatase inhibitor cocktail (Thermo Scientific, catalog# 78441) at 1:100 dilution. Each sample was vortexed for 15 s and then incubated for 1 h at 4^{o}C, with vortexing every 15 min. Each tube was then spun at 13,000 rpm for 1 min after which the lysate was transferred to a new tube. Each lysate sample was mixed with equal volume of 2x western blot loading buffer treated with beta-mercaptoethanol at 1:50 dilution and 40 µl was loaded in each well. The samples were then incubated at 95^{o}C for 5 min. The gel was run at 150 V for 1.5 h, then transferred to nitrocellulose membrane run at 100 V for 1 h and blocked by incubating the plate with 10 ml of blocking buffer (5% milk powder in 1xPBST) at room temperature (RT) for 1 h with shaking. Then the membrane was washed with 1x PBST three times for 5 min each with shaking at RT and incubated overnight with shaking at 4^{o}C with respective primary antibodies prepared in 5% milk blocking buffer. Following primary antibodies were used: anti-Flag mouse monoclonal 1^{o} Ab against flag tagged ZMPSTE24 (9A3) (Cell Signaling Technology, cat. no. 8146S) at 1:1000 dilution, anti-PRRSV SR-30 1^{o} monoclonal Ab (provided by Dr. Eric Nelson) at 1:300 dilution, and mouse monoclonal anti-beta actin-Ab (Sigma-Aldrich, catalog# A2228) at 1:5000 dilution. Next day, the membrane was washed with 1x PBST three times and then incubated while shaking at RT in dark with Goat anti-Mouse IRDye® conjugated 2^{o} Ab (LI-COR, catalog# 926-32210) diluted to 1:5000 in 1x PBST. The membrane was washed in 1x PBST and observed using LI-COR Odyssey Infrared Imaging System. Quantification of the protein (band) intensity was performed using Image J. Beta-actin house keeping gene was used to calculate relative fold change in

PRRSV N protein expression in ZMPSTE24 overexpressing cells as compared to vector control cells.

3.3.4 Immunofluorescence staining and flow cytometry

Briefly, MARC-145 cells were transfected with either vector control pCMV-3Tag-8 or FLAG-tagged ZMPSTE24 cloned into pCMV-3Tag-8 (ZMPSTE24-FLAG) [43] in triplicate wells of a 24-well plate as described earlier. Then 72 h post transfection, PRRSV 23983 was added at an MOI of 1 to all six wells in DMEM growth medium and the plate was incubated at 37^{o}C for 24 h. All wells were fixed with 80% acetone at RT for 20 min, followed by air drying. Then 350 µl per well of 1:80 diluted FITC conjugated anti-PRRSV Ab specific to N protein (SDOW-17) (provided by Dr. Eric Nelson) was added and incubated at 37^{o}C for 1 h. Cells in each well were washed in 1x PBS and then observed under immunofluorescence microscope. Next, cells in each well were scraped in 500 µl PBS, analyzed by flow cytometry, and mean fluorescence intensity for FITC staining was calculated. The images were captured at 10x magnification using an Olympus IX70 Inverted-Microscope (Epi-fluorescence and phase contrast).

3.3.5 Immunofluorescence staining and confocal microscopy

In duplicate wells, cells were transfected with either vector control pCMV-3Tag-8 or ZMPSTE24-FLAG in two 8-chamber slides following the protocol as described earlier. For 3 hpi study, PRRSV 23983 at an MOI of 4 was added to each well of the first slide except one vector-control transfected well. For 24 hpi study, PRRSV 23983 at an MOI of 1 was added to each well of the second slide. Then the two 8-chamber slides were fixed in 3.8% formaldehyde for 10 min at RT followed by one wash in 1x PBS for 5 min. The cells in each well were then treated with 0.2% Triton x-100 diluted in 1x PBS for permeabilization and incubated at RT for 10 min. Next, the cells were washed and

incubated at RT for 30 min with 5% goat serum in PBS for blocking non-specific antibody binding. After washing in 1x PBS, cells in each well were incubated overnight at RT with primary antibody diluted in 5% goat serum. Mouse monoclonal anti-Flag primary antibody against flag tagged ZMPSTE24 (9A3) (Cell Signaling Technology, cat. no. 8146S) was added at 1:1600 dilution to all wells except the uninfected vector-control transfected well to which 5% goat serum was added. Next day, the slides were washed three times with 1x PBS and then incubated for 1 h at 37^{o}C with the secondary antibody. To the three wells incubated with anti-Flag primary antibody, Alexa fluor 647 conjugated goat anti-mouse IgG 2^{o} Ab (Abcam) at 1:200 dilution was added. After 1 h incubation, anti-PRRSV FITC conjugated Ab (SDOW-17) at 1:80 dilution was added and cells were incubated at 37^{o}C for 1 h. The uninfected vector-control transfected well was incubated with Alexafluor 647 2^{o} Ab only. The slides were washed in 1x PBS, counterstained with DAPI for 3 min, air dried and then mounted using ProLong Gold antifade mounting reagent (Invitrogen). The slide was then stored at 4^{o}C overnight and then observed using Olympus Fluoview FV1200 Laser Scanning Confocal Microscope to study colocalization of PRRSV and ZMPSTE24 at 3 or 24 hpi. Briefly, five different microscopic fields at 40x magnification were analyzed by confocal microscopy for each vector control transfected group and ZMPSTE24 transfected group at each time point. In each field, cells were counted by DAPI staining and then the percentage of cells staining for PRRSV (green) or ZMPSTE24 (red) was calculated. Colocalization study was performed by counting the number of DAPI stained cells with yellow fluorescence which is observed due to overlap of the emission spectra for green (FITC conjugated Ab for PRRSV N at 488 wavelength) and red (Alexafluor 647 conjugated Ab for ZMPSTE24) dyes.

Uninfected control cells stained with FITC conjugated anti-PRRSV Ab were used as a control for comparing the background (green) staining to the PRRSV infected group. All images were taken at 40x magnification.

3.3.6 Real-time reverse transcription PCR (RT-PCR)

Total RNA extraction was carried out from cells harvested as described earlier using RNeasy Mini Kit (Qiagen Cat. No. 74104) according to the manufacturer's protocol. To generate cDNA, 1 µg of the total RNA extracted was reversed transcribed using High Capacity cDNA Reverse Transcription Kit (applied biosystems) under following reaction conditions: 25°C for 10 min, 37°C for 120 min, and 85°C for 5 min (Applied Biosystems GeneAmp PCR System 2400). Real time PCR was performed by using 3 µl of the cDNA product as a template for each reaction using Brilliant II SYBR Green QPCR master mix (Agilent Technologies). Forty cycles of following conditions were used: 95°C for 10 min, 95°C for 30 s, 55°C for 30 s, and 72°C for 30 s. Primers specific to beta-actin housekeeping gene, PRRSV N and ZMPSTE24 are shown in Table 3.1. The reactions were run in a QuantStudio 6 Flex Real-Time PCR System (Applied Biosystems). Data analysis was performed by calculating the mean fold change in gene expression using the ΔΔCT method. House keeping gene beta-actin was used as a reference gene for comparing the fold change between two treatment groups [88].

3.3.7 $TCID_{50}$ titer

Fifty-percent tissue culture infectious dose ($TCID_{50}$) assay was performed to determine the infectious PRRSV 23983 titer in the supernatant at 24 hpi obtained from the previously described ZMPSTE24 overexpression or siRNA induced knockdown experiments. $TCID_{50}$ titer was determined using the Spearman-Karber method [79].

3.3.8 Cytotoxicity assay

MARC-145 cells were seeded in a 96-well plate at $1x10^4$ cells/well and incubated at 37°C for 24 h. Then, cells were transfected with either the vector control pCMV-3Tag-8 or ZMPSTE24-FLAG, or negative control siRNA (Ambion, cat. no. AM4642) or ZMPSTE24 siRNA (Life technologies, siRNA ID# s20067) in triplicate wells, as described earlier. Then 72 h post transfection, each well of the 96-well plate incubated with 200 µl of DMEM growth medium was treated with 10 µl of CCK-8 solution (Sigma, cat. no. 96992) and incubated at 37°C for 3 h, after which absorbance was measured at 450 nm using a Synergy 2 plate reader (BioTek).

3.3.9 Statistical analysis

Student's t-test (two tailed) was used to compare the PRRSV titer between ZMPSTE24 overexpressing cells and vector control transfected cells. Likewise, PRRSV titer was compared between siRNA induced ZMPSTE24 silenced cells and control siRNA silenced cells. Similarly, mean fluorescence intensity between the ZMPSTE24 overexpressing cells and vector control cells was compared. A p value<0.05 was considered as statistically significant. Data are represented as mean of three independent experiments ± standard deviation.

Table 3.1 Primer sequences of ZMPSTE24, PRRSV N and the housekeeping gene.

Gene	**Forward Primer (FP) 5′-3′**	**Reverse Primer (RP) 5′-3′**
beta-actin	TTGCTGACAGGATGCAGAAGGAGA	ACTCCTGCTTGCTGATCCACATCT
ZMPSTE24	GAGGAAGAAGGGAACAGTGAA	ATGGCCTAGTACAGCGAGTA
PRRSV N	GTCAATCCAGACCGCCTTTA	GATCAGGCGCACAGTATGAT

3.4 Results

3.4.1 Overexpression of ZMPSTE24 in MARC-145 cells reduces PRRSV replication

Western blot confirmed the expression of ZMPSTE24 protein in cells transfected with pCMV-3Tag-8 plasmid expressing ZMPSTE24-FLAG but not in vector control pCMV-3Tag-8 transfected cells (Fig. 3.1A). A lower level of expression of PRRSV N protein was observed in ZMPSTE24 overexpressing cells as compared to the vector control cells at 24 hpi (Fig. 3.1A). An average of 3% reduction in PRRSV N protein expression in ZMPSTE24 overexpressing cells was confirmed by quantification of the protein band intensity (Fig. 3.1B). $TCID_{50}$ assay showed an average of 146-fold decrease (2.16 log reduction) in virus titer in ZMPSTE24 overexpressing cells as compared to the vector control transfected cells (Fig. 3.1C). Further, Immunofluorescence staining showed fewer virus positive staining (green) in ZMPSTE24 overexpressing cells as compared to the vector control transfected cells (Fig. 3.1D). A significant reduction in mean fluorescence intensity ($p<0.05$) was observed in ZMPSTE24 overexpressing MARC-145 cells as compared to the vector control cells at 24 hpi as confirmed by flow

cytometry (Fig. 3.1E). No significant difference in cell viability between vector control and ZMPSTE24 containing plasmid transfected cells was observed at 72 h post-transfection as measured using CCK-8 cell viability assay (Fig. 3.1F). The mean absorbance values of 1.64 and 1.55 were confirmed in vector control and ZMPSTE24 overexpressing cells respectively (Fig. 3.1F).

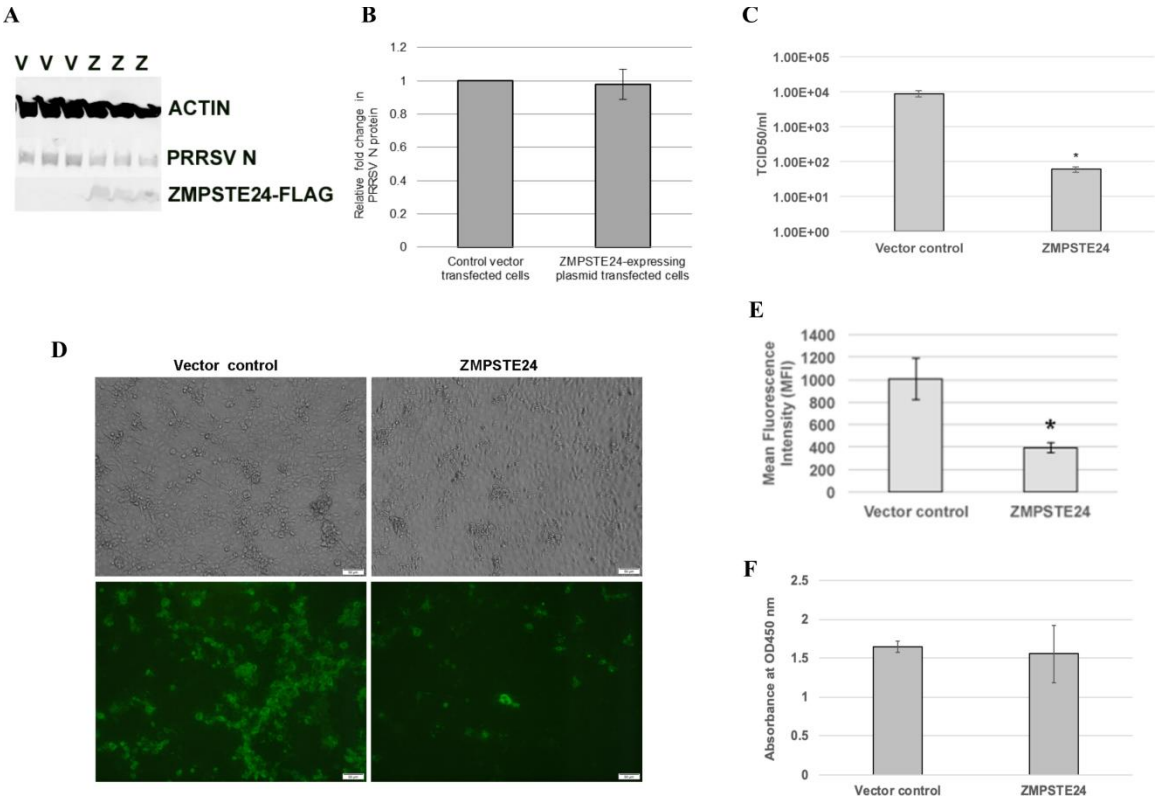

Fig. 3.1 Over-expression of ZMPSTE24 in MARC-145 cells reduces PRRSV replication. Standard deviation and mean of three replicates are shown for each graph. **A:** Western blot analysis showing the expression of ZMPSTE24 in cells transfected with ZMPSTE24 expressing plasmid. Lanes 1-3 were transfected with pCMV-3Tag-8 vector control (V) while wells 4-6 were transfected with pCMV-3Tag-ZMPSTE24-FLAG (Z). Beta-actin was used as a loading control. The expression of PRRSV N protein is shown. **B:** Quantification of the protein band intensity using Image J showed an average of 3% reduction in PRRSV N protein expression in ZMPSTE24 overexpressing cells. **C:** Virus titers in the supernatants of PRRSV infected cells at 24 hpi. * indicates $p < 0.05$. **D:** Immunofluorescence staining of virus-infected cells at 24 hpi. Top panel shows the bright field image and the lower panel shows PRRSV positive staining. **E:** Flow cytometry analysis of virus-infected cells at 24 hpi. * indicates $p < 0.05$. **F:** CCK-8 assay was used to compare cell viability between vector control and ZMPSTE24 containing plasmid transfected cells. No significant difference ($p > 0.05$) was observed.

3.4.2 Silencing of endogenous ZMPSTE24 slightly affects PRRSV replication

An average of 74% knockdown of endogenous ZMPSTE24 gene was achieved, as confirmed by RT-PCR (Fig. 3.2A). Further, RT-PCR showed an average of 1.2 fold increase in PRRSV N gene transcript relative to the silencing control (Fig. 3.2B). Surprisingly, virus titers in the supernatants of ZMPSTE24 knockdown cells showed a slight decrease relative to control silenced cells. An average of 2.5 fold decrease in virus titer was observed (Fig. 3.2C). There was no significant difference in cell viability between negative control siRNA and ZMPSTE24 siRNA transfected groups (Fig. 3.2D). CCK-8 cell viability assay gave mean absorbance values of 1.76 and 1.99 in negative control siRNA and ZMPSTE24 siRNA induced silenced cells respectively (Fig. 3.2D).

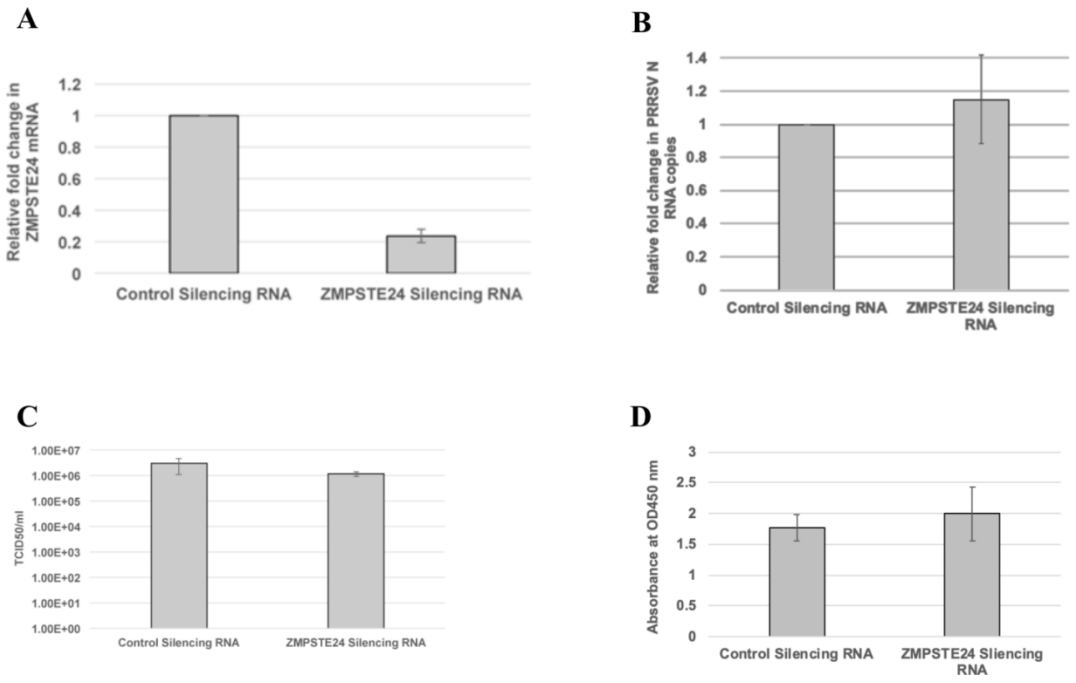

Fig. 3.2 Silencing of endogenous ZMPSTE24 slightly affects PRRSV replication. Standard deviation and mean of three replicates are shown for each graph. **A:** qRT-PCR showed an average ZMPSTE24 knockdown efficiency of 74%. **B:** The relative fold change in viral RNA copies in ZMPSTE24 siRNA transfected cells compared to control silencing RNA transfected cells. No significant difference ($p > 0.05$) was observed between the two groups. **C:** $TCID_{50}$ assay showing virus titers in the supernatants of ZMPSTE24 silencing cells as compared to the control silencing cells. No significant difference between the two groups was observed ($p > 0.05$). **D:** Cell viability was not significantly ($p > 0.05$) affected by the transient silencing of ZMPSTE24.

3.4.3 Over-expression of ZMPSTE24 does not affect PRRSV entry into MARC-145 cells

There were no significant differences in the number of PRRSV positive cells or total viral RNA copies between the vector control and ZMPSTE24 over-expressing cells at 3 hpi (Fig. 3.3A, B). RT-PCR showed 900 fold change in ZMPSTE24 mRNA

transcript in ZMPSTE24 overexpressing MARC-145 cells as compared to vector control transfected cells, confirming the successful transfection and over-expression of ZMPSTE24 (Fig. 3.3C). Extensive colocalization between PRRSV and ZMPSTE24 was observed at 3 hpi. However, little or no colocalization was observed at 24 hpi (Fig. 3.3D).

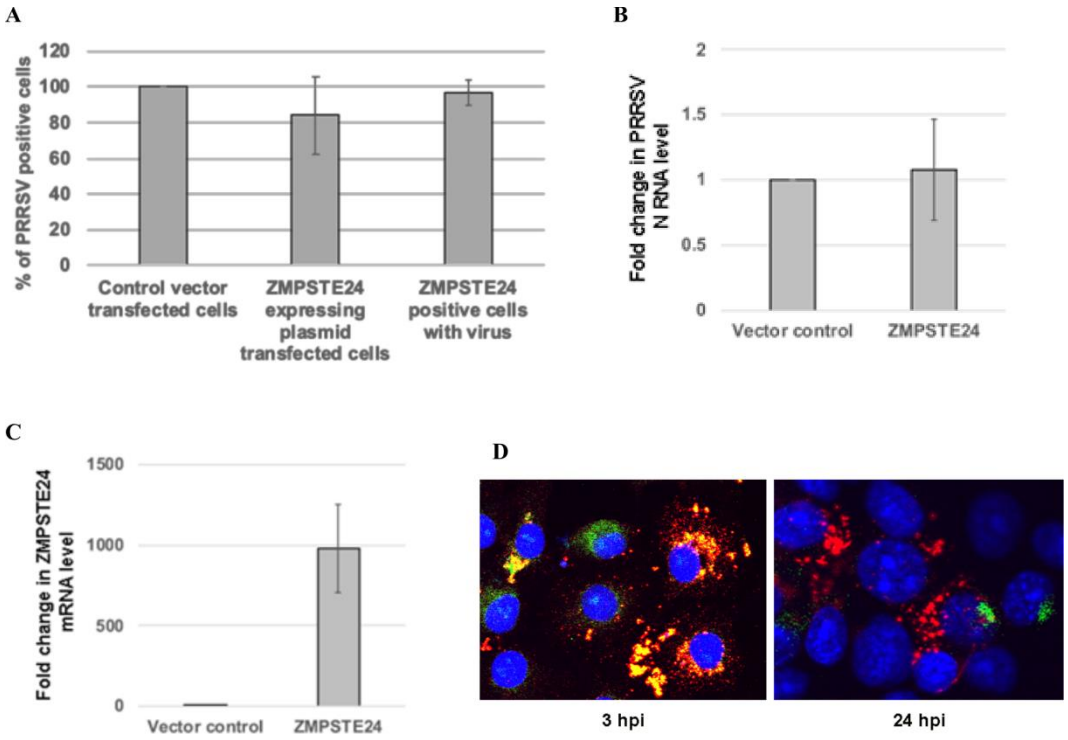

Fig. 3.3 Over-expression of ZMPSTE24 does not affect PRRSV entry into MARC-145 cells. **A:** Quantitative analysis of PRRSV positive cells in ZMPSTE24 expressing cells and vector control cells at 3 hpi. Percentage of PRRSV positive cells was determined by dividing the green (FITC-SDOW-17) staining cells by total number of cells (DAPI stained, blue) in each microscopic field. The average and standard deviations of five different microscopic fields are shown. The percentage of red staining (Alexa 647, ZMPSTE24 expressing cells) that is positive for PRRSV was determined similarly. Red and green co-staining cells were counted and divided by the total number of red staining cells. No significant difference ($p > 0.05$) was observed between vector control and ZMPSTE24 transfected group. **B:** The relative fold change in viral RNA copies in ZMPSTE24 transfected cells when compared to vector control at 3 hpi as determined by qRT-PCR. Standard deviation and mean of three replicates are shown. **C:** qRT-PCR showing the relative fold increase in ZMPSTE24 mRNA level in ZMPSTE24 transfected cells compared to vector control cells. Standard deviation and mean of three replicates are shown. **D:** Colocalization of PRRSV N protein with exogenous ZMPSTE24. Representative images show the extensive colocalization of PRRSV N with ZMPSTE24 at 3 hpi and little or no colocalization of PRRSV N protein with ZMPSTE24 at 24 hpi. Green: PRRSV N protein. Red: Flag-tagged ZMPSTE24. Blue: DAPI nuclei.

3.5 Discussion

ZMPSTE24 overexpression has been shown to significantly reduce influenza A virus (IAV) infection in A549 cells [43]. Interestingly, in the same study, although ZMPSTE24 inhibited several RNA and DNA viruses requiring pH dependent fusion, it failed to inhibit murine leukemia virus [43]. To investigate the effect of ZMPSTE24 on PRRSV replication, we first employed the ZMPSTE24 overexpression system. In our

study, we confirmed reduced expression of PRRSV N protein as well as reduced virus titer in ZMPSTE24 overexpressing cells. Further, cell viability did not play a role in ZMPSTE24 mediated PRRSV restriction. To further confirm the role of ZMPSTE24 in restricting PRRSV replication, we employed silencing RNA mediated knockdown of endogenous ZMPSTE24 approach. The PRRSV N gene transcripts were only slightly higher in ZMPSTE24 silenced cells relative to silencing control. Overall, our results showed that silencing of endogenous ZMPSTE24 does not appear to have a significant impact on PRRSV replication. This observation could be due to the knockdown efficiency (74%) achieved in our hands, while previous studies used cells derived from gene knockout animals [43]. Additionally, it is possible that transient silencing of ZMPSTE24 may not mimic the cells from gene knockout mice [43, 77]. Taken together, both overexpression and RNA silencing of ZMPSTE24 data suggest its antiviral effect against PRRSV.

Previous studies showed that ZMPSTE24 and IFITM3 work together to block entry of various enveloped viruses including IAV and arenaviruses [43, 123]. In this study, we investigated if overexpression of ZMPSTE24 restricts PRRSV entry. There were no significant differences ($p > 0.05$) in the number of PRRSV positive cells or total viral RNA copies between the vector control and ZMPSTE24 over-expressing cells at 3 hpi. Our results are in indirect contrast to an earlier study which showed a dramatic lower number of IAV virus positive cells compared to the vector control as early as 2 hpi and persisted until 8 hpi [43]. This difference could be due to different virus entry mechanisms or distinctive replication efficiency of each virus in the respective cell culture model systems.

PRRSV completes one infectious cycle in about 8 h [153]. We observed that PRRSV more significantly colocalized with the early endosome marker EEA1 at 3 hpi, but most disappeared from early endosome at 6 hpi (data not shown). Relatively fewer PRRSV colocalized with LAMP-1, a marker of late endosome/lysosome, during the first 6 hpi. One previous study showed colocalization of PRRSV with EEA1 but not with the late endosomal marker [131]. However, a more recent study showed colocalization of PRRSV with late endosome marker [153]. Therefore, the existing data remain controversial regarding whether PRRSV enters cells through late endosomes. We observed extensive colocalization between ZMPSTE24 and PRRSV at 3 hpi, suggesting virus entry into early endosomes was not disturbed by ZMPSTE24 overexpression. However, little or no colocalization between PRRSV and ZMPSTE24 was observed at 24 hpi, suggesting that restriction of PRRSV replication in cells with ZMPSTE24 overexpression likely occurred after 3 hpi. It is known that IFITM3 and ZMPSTE24 work together to trap enveloped virus in the endolysosomal compartment for degradation [43, 84]. Future studies on colocalization of PRRSV with late endosome/lysosome marker (LAMP-1) in ZMPSTE24 overexpressing cells may reveal more information on whether PRRSV is also being degraded in late endosome/lysosome.

We observed a difference in the morphology of virus infected cells between the cells not expressing ZMPSTE24 and the cells over-expressing ZMPSTE24. Specifically, an increased number of cell surface protrusions were observed in the vector control group at 3 hpi (data not shown). One possible explanation is that ZMPSTE24 overexpression may suppress the formation of cell surface protrusions mediated by small GTPase such as Rho [50, 75, 101]. Future investigation may clarify if ZMPSTE24 also interferes with

PRRSV intercellular spread. Overall, the data suggest that overexpression of ZMPSTE24 does not significantly impact virus entry and may limit virus replication via a post-entry step. Although ZMPSTE24 inhibited several RNA and DNA viruses requiring pH dependent fusion, it failed to inhibit murine leukemia virus [43]. Alternatively, ZMPSTE24 may also bind to other substrates for its antiviral activity [84]. The detailed mechanism by which overexpression of ZMPSTE24 restricts PRRSV replication needs to be examined in future studies.

In conclusion, overexpression of ZMPSTE24 reduced PRRSV infection in MARC-145 cells. There was no significant difference in the percentage of cells positive for PRRSV and viral RNA copies in ZMPSTE24 overexpressing cells as compared to the vector control cells at 3 hpi. This suggests that ZMPSTE24 may inhibit PRRSV at a post-entry step. The role of endogenous ZMPSTE24 in PRRSV replication seems to be limited in our experimental model system and needs to be investigated further in future studies.

Acknowledgments

This study is partly supported by Animal Health and Production and Animal Products: Animal Health and Disease (grant no. 2021-67016-34460/project accession no. 1025717) from the USDA National Institute of Food and Agriculture (NIFA) and Hatch (SD00H660-19) and Hatch Multi State (SD00R656-16) from USDA NIFA and South Dakota Agricultural Experiment Station.

Author Contributions

XW designed the study, analyzed the data, and wrote the manuscript. PK conducted experiments, analyzed the results and wrote the manuscript. EN and SL provided reagents/analytic tools. MH contributed to confocal microscopy and analysis.

Conflicts of Interest

The authors declare no conflict of interest.

Chapter 4: Conclusions and Future directions

In this study, the role of IFITM3 on PRRSV replication was studied. Our overexpression experiments support the antiviral role of IFITM3 against PRRSV. Surprisingly, siRNA induced silencing of endogenous IFITM3 in MARC-145 cells only showed a slight enhancement on PRRSV replication. However, a recent study showed significant enhancement of PRRSV infection upon silencing of endogenous IFITM3 [153]. The discrepancy in results could be due to different knockdown efficiency since we only achieved an average of 50% knockdown under our experimental conditions. The antiviral role of ZMPSTE24, a downstream effector of IFITM3, was also studied. Our study showed that ZMPSTE24, like IFITM3, exerts antiviral effect against PRRSV. However, silencing of ZMPSTE24 at a knockdown efficiency of 74% showed only slight effect on PRRSV replication. In an earlier study, ZMPSTE24 knockout mouse embryonic fibroblasts (MEFs) were shown to be highly susceptible to Influenza A virus (IAV) infection. The transient silencing of ZMPSTE24 in our study may be one of the factors contributing to the limited effect of silencing ZMPSTE24 on PRRSV restriction. Taken together, the results from our study suggest that the endogenous proteins-IFITM3 and ZMPSTE24 only play a small role in PRRSV replication under the experimental conditions used in our study.

The viruses that enter into host cells via late endosomes and are pH dependent are shown to be restricted by IFITM3 at the virus entry step. Amphotericin B treatment can fully restore virus replication. Earlier study showed that PRRSV requires trafficking through early endosomes only [131]. However, a recent study suggests that PRRSV is trafficked into IFITM3 containing endosomes and lysosomes [153]. Zhang et al. further

showed that cholesterol accumulation blocks virus membrane fusion. Our results also suggest that PRRSV is trafficked to late endosomes, even though greater percentage of colocalization occurred with early endosomes (at 3 hpi) than with late endosomes. Consistent with this observation, it is interesting that Amphotericin B only partially restored PRRSV replication in our study. Further, our study suggested that PRRSV was more significantly inhibited after 3 hpi. PRRSV was detected in IFITM3 overexpressing cells at both 3 and 24 hpi, suggesting that IFITM3 did not completely restrict virus entry and replication. Previous study has shown that ZMPSTE24 impedes IAV endosomal entry [43]. In our study, while little or no colocalization between PRRSV and ZMPSTE24 was observed at 24 hpi, significant colocalization was observed at 3 hpi. There was no significant difference in the percentage of PRRSV positive cells between vector control and ZMPSTE24 overexpressing cells at 3 hpi. Collectively, these findings suggest that IFITM3 and ZMPSTE24 likely restrict PRRSV at multiple post-entry steps.

ZMPSTE24 and IFITM3 work together to impede virus-host membrane fusion primarily in the late endosomes. In future, it will be important to investigate if PRRSV is also trapped in the endolysosomes for degradation. Studying colocalization of PRRSV with late endosome marker in ZMPSTE24 overexpressing cells may reveal more on this. The restriction factor, ZMPSTE24 was proposed to be a downstream effector of IFITM3 protein and was shown to be important in the IFITM3 mediated restriction of IAV [43]. It may be useful to test if knockdown of IFITM3 affects endosomal recruitment of ZMPSTE24 and not vice versa. However, ZMPSTE24 may also restrict PRRSV by IFITM3 independent mechanisms. In our study, we showed that the restriction factors-IFITM3 and ZMPSTE24 individually restrict PRRSV replication in vitro. In future, it

may be important to investigate the cooperative antiviral activity of IFITM3 and ZMSPTE24 against PRRSV. For instance, the synergistic effect of IFITM3 and ZMPSTE24 against PRRSV replication could be investigated. Interestingly, a recent study on arenaviruses, known to be relatively resistant to the effect of IFITM3, showed that ZMPSTE24 overexpression causes redistribution of IFITM3 to distinct endosomal compartments, such as early endosomes [123]. Overall, these findings may have important implication in the context of PRRSV restriction and needs further study.

References

1. Akira S, Uematsu S, Takeuchi O (2006) Pathogen recognition and innate immunity. Cell 124:783-801
2. Allende R, Lewis TL, Lu Z, Rock DL, Kutish GF, Ali A, Doster AR, Osorio FA (1999) North American and European porcine reproductive and respiratory syndrome viruses differ in non-structural protein coding regions. The Journal of general virology 80 (Pt 2):307-315
3. Amini-Bavil-Olyaee S, Choi Youn J, Lee Jun H, Shi M, Huang IC, Farzan M, Jung Jae U (2013) The Antiviral Effector IFITM3 Disrupts Intracellular Cholesterol Homeostasis to Block Viral Entry. Cell host & microbe 13:452-464
4. Bailey CC, Huang IC, Kam C, Farzan M (2012) Ifitm3 limits the severity of acute influenza in mice. PLoS pathogens 8:e1002909-e1002909
5. Bailey CC, Kondur HR, Huang IC, Farzan M (2013) Interferon-induced transmembrane protein 3 is a type II transmembrane protein. J Biol Chem 288:32184-32193
6. Bailey CC, Zhong G, Huang IC, Farzan M (2014) IFITM-Family Proteins: The Cell's First Line of Antiviral Defense. Annu Rev Virol 1:261-283
7. Barnard P, McMillan NAJ (1999) The Human Papillomavirus E7 Oncoprotein Abrogates Signaling Mediated by Interferon-α. Virology 259:305-313
8. Barrowman J, Michaelis S (2009) ZMPSTE24, an integral membrane zinc metalloprotease with a connection to progeroid disorders. Biological chemistry 390:761-773
9. Barrowman J, Hamblet C, Kane MS, Michaelis S (2012) Requirements for efficient proteolytic cleavage of prelamin A by ZMPSTE24. PloS one 7:e32120
10. Basters A, Knobeloch K-P, Fritz G (2018) USP18 - a multifunctional component in the interferon response. Biosci Rep 38:BSR20180250
11. Bautista EM, Goyal SM, Collins JE (1993) Serologic survey for Lelystad and VR-2332 strains of porcine respiratory and reproductive syndrome (PRRS) virus in US swine herds. Journal of veterinary diagnostic investigation : official publication of the American Association of Veterinary Laboratory Diagnosticians, Inc 5:612-614
12. Bautista EM, Goyal SM, Yoon IJ, Joo HS, Collins JE (1993) Comparison of porcine alveolar macrophages and CL 2621 for the detection of porcine reproductive and respiratory syndrome (PRRS) virus and anti-PRRS antibody. Journal of veterinary diagnostic investigation : official publication of the American Association of Veterinary Laboratory Diagnosticians, Inc 5:163-165
13. Bergo MO, Gavino B, Ross J, Schmidt WK, Hong C, Kendall LV, Mohr A, Meta M, Genant H, Jiang Y, Wisner ER, Van Bruggen N, Carano RA, Michaelis S, Griffey SM, Young SG (2002) Zmpste24 deficiency in mice causes spontaneous bone fractures, muscle weakness, and a prelamin A processing defect. Proceedings of the National Academy of Sciences of the United States of America 99:13049-13054
14. Beura LK, Sarkar SN, Kwon B, Subramaniam S, Jones C, Pattnaik AK, Osorio FA (2010) Porcine reproductive and respiratory syndrome virus nonstructural protein 1beta modulates host innate immune response by antagonizing IRF3 activation. Journal of virology 84:1574-1584

15. Bradbury LE, Kansas GS, Levy S, Evans RL, Tedder TF (1992) The CD19/CD21 signal transducing complex of human B lymphocytes includes the target of antiproliferative antibody-1 and Leu-13 molecules. Journal of immunology (Baltimore, Md : 1950) 149:2841-2850
16. Brass AL, Huang IC, Benita Y, John SP, Krishnan MN, Feeley EM, Ryan BJ, Weyer JL, van der Weyden L, Fikrig E, Adams DJ, Xavier RJ, Farzan M, Elledge SJ (2009) The IFITM proteins mediate cellular resistance to influenza A H1N1 virus, West Nile virus, and dengue virus. Cell 139:1243-1254
17. Brodsky LI, Wahed AS, Li J, Tavis JE, Tsukahara T, Taylor MW (2007) A novel unsupervised method to identify genes important in the anti-viral response: application to interferon/ribavirin in hepatitis C patients. PloS one 2:e584-e584
18. Buddaert W, Van Reeth K, Pensaert M (1998) In Vivo and In Vitro Interferon (IFN) Studies with the Porcine Reproductive and Respiratory Syndrome Virus (PRRSV). In: Enjuanes L, Siddell SG, Spaan W (eds) Coronaviruses and Arteriviruses. Springer US, Boston, MA, pp 461-467
19. Calvert JG, Slade DE, Shields SL, Jolie R, Mannan RM, Ankenbauer RG, Welch SK (2007) CD163 expression confers susceptibility to porcine reproductive and respiratory syndrome viruses. Journal of virology 81:7371-7379
20. Capell BC, Collins FS (2006) Human laminopathies: nuclei gone genetically awry. Nature reviews Genetics 7:940-952
21. Chae C (2016) Porcine respiratory disease complex: Interaction of vaccination and porcine circovirus type 2, porcine reproductive and respiratory syndrome virus, and Mycoplasma hyopneumoniae. Veterinary journal (London, England : 1997) 212:1-6
22. Chambers R, Takimoto T (2009) Antagonism of innate immunity by paramyxovirus accessory proteins. Viruses 1:574-593
23. Chemudupati M, Kenney AD, Bonifati S, Zani A, McMichael TM, Wu L, Yount JS (2019) From APOBEC to ZAP: Diverse mechanisms used by cellular restriction factors to inhibit virus infections. Biochimica et biophysica acta Molecular cell research 1866:382-394
24. Chen Z, Lawson S, Sun Z, Zhou X, Guan X, Christopher-Hennings J, Nelson EA, Fang Y (2010) Identification of two auto-cleavage products of nonstructural protein 1 (nsp1) in porcine reproductive and respiratory syndrome virus infected cells: nsp1 function as interferon antagonist. Virology 398:87-97
25. Christianson WT, Choi CS, Collins JE, Molitor TW, Morrison RB, Joo HS (1993) Pathogenesis of porcine reproductive and respiratory syndrome virus infection in mid-gestation sows and fetuses. Canadian journal of veterinary research = Revue canadienne de recherche veterinaire 57:262-268
26. Darnell JE, Jr., Kerr IM, Stark GR (1994) Jak-STAT pathways and transcriptional activation in response to IFNs and other extracellular signaling proteins. Science (New York, NY) 264:1415-1421
27. Das PB, Dinh PX, Ansari IH, de Lima M, Osorio FA, Pattnaik AK (2010) The minor envelope glycoproteins GP2a and GP4 of porcine reproductive and respiratory syndrome virus interact with the receptor CD163. Journal of virology 84:1731-1740

28. Delputte PL, Vanderheijden N, Nauwynck HJ, Pensaert MB (2002) Involvement of the matrix protein in attachment of porcine reproductive and respiratory syndrome virus to a heparinlike receptor on porcine alveolar macrophages. Journal of virology 76:4312-4320
29. Delputte PL, Van Breedam W, Barbé F, Van Reeth K, Nauwynck HJ (2007) IFN-α Treatment Enhances Porcine Arterivirus Infection of Monocytes via Upregulation of the Porcine Arterivirus Receptor Sialoadhesin. Journal of Interferon & Cytokine Research 27:757-766
30. Deng MC, Chang CY, Huang TS, Tsai HJ, Chang C, Wang FI, Huang YL (2015) Molecular epidemiology of porcine reproductive and respiratory syndrome viruses isolated from 1991 to 2013 in Taiwan. Archives of virology 160:2709-2718
31. Desai TM, Marin M, Chin CR, Savidis G, Brass AL, Melikyan GB (2014) IFITM3 restricts influenza A virus entry by blocking the formation of fusion pores following virus-endosome hemifusion. PLoS pathogens 10:e1004048
32. Done SH, Paton DJ, White ME (1996) Porcine reproductive and respiratory syndrome (PRRS): a review, with emphasis on pathological, virological and diagnostic aspects. Br Vet J 152:153-174
33. Duan X, Nauwynck HJ, Favoreel HW, Pensaert MB (1998) Identification of a putative receptor for porcine reproductive and respiratory syndrome virus on porcine alveolar macrophages. Journal of virology 72:4520-4523
34. Espert L, Degols G, Gongora C, Blondel D, Williams BR, Silverman RH, Mechti N (2003) ISG20, a new interferon-induced RNase specific for single-stranded RNA, defines an alternative antiviral pathway against RNA genomic viruses. J Biol Chem 278:16151-16158
35. Everitt AR, Clare S, Pertel T, John SP, Wash RS, Smith SE, Chin CR, Feeley EM, Sims JS, Adams DJ, Wise HM, Kane L, Goulding D, Digard P, Anttila V, Baillie JK, Walsh TS, Hume DA, Palotie A, Xue Y, Colonna V, Tyler-Smith C, Dunning J, Gordon SB, Everingham K, Dawson H, Hope D, Ramsay P, Walsh TS, Campbell A, Kerr S, Harrison D, Rowan K, Addison J, Donald N, Galt S, Noble D, Taylor J, Webster N, Taylor I, Aldridge J, Dornan R, Richard C, Gilmour D, Simmons R, White R, Jardine C, Williams D, Booth M, Quasim T, Watson V, Henry P, Munro F, Bell L, Ruddy J, Cole S, Southward J, Allcoat P, Gray S, McDougall M, Matheson J, Whiteside J, Alcorn D, Rooney K, Sundaram R, Imrie G, Bruce J, McGuigan K, Moultrie S, Cairns C, Grant J, Hughes M, Murdoch C, Davidson A, Harris G, Paterson R, Wallis C, Binning S, Pollock M, Antonelli J, Duncan A, Gibson J, McCulloch C, Murphy L, Haley C, Faulkner G, Freeman T, Hume DA, Baillie JK, Chaussabel D, Adamson WE, Carman WF, Thompson C, Zambon MC, Aylin P, Ashby D, Barclay WS, Brett SJ, Cookson WO, Drumright LN, Dunning J, Elderfield RA, Garcia-Alvarez L, Gazzard BG, Griffiths MJ, Habibi MS, Hansel TT, Herberg JA, Holmes AH, Hussell T, Johnston SL, Kon OM, Levin M, Moffatt MF, Nadel S, Openshaw PJ, Warner JO, Aston SJ, Gordon SB, Hay A, McCauley J, O'Garra A, Banchereau J, Hayward A, Kellam P, Baillie JK, Hume DA, Simmonds P, McNamara PS, Semple MG, Smyth RL, Nguyen-Van-Tam JS, Ho LP, McMichael AJ, Kellam P, Smyth RL, Openshaw PJ, Dougan G, Brass AL, Kellam P, The Gen II, Critical Care

Medicine UoE, Generation Scotland UoEMMC, Intensive Care National A, Research Centre L, Intensive Care Unit ARI, Intensive Care Unit AH, Intensive Care Unit BGHM, Intensive Care Unit CHK, Intensive Care Unit D, Galloway Royal I, Intensive Care Unit GRI, Intensive Care Unit HHL, Intensive Care Unit IRHG, Intensive Care Unit MHA, Intensive Care Unit NHD, Intensive Care Unit QMHD, Intensive Care Unit RHI, Intensive Care Unit RAHP, Intensive Care Unit SGHG, Intensive Care Unit SJsHL, Intensive Care Unit SRI, Intensive Care Unit SHG, Intensive Care Unit VHG, Intensive Care Unit WGHE, Intensive Care Unit WIG, Wellcome Trust Clinical Research Facility E, Roslin Institute UoE, The MI, Benaroya Research Institute USA, Gartnavel General Hospital GGUK, Health Protection Agency UK, Imperial College London UK, Liverpool School of Tropical Medicine UK, National Institute for Medical Research UK, Roche NUSA, University College London UK, University of Edinburgh UK, University of Liverpool UK, University of Nottingham UK, University of Oxford UK, Wellcome Trust Sanger Institute UK (2012) IFITM3 restricts the morbidity and mortality associated with influenza. Nature 484:519-523

36. Faaberg KS, Hocker JD, Erdman MM, Harris DLH, Nelson EA, Torremorell M, Plagemann PGW (2006) Neutralizing Antibody Responses of Pigs Infected with Natural GP5 N-Glycan Mutants of Porcine Reproductive and Respiratory Syndrome Virus. Viral immunology 19:294-304
37. Fabriek BO, Dijkstra CD, van den Berg TK (2005) The macrophage scavenger receptor CD163. Immunobiology 210:153-160
38. Fang Y, Snijder EJ (2010) The PRRSV replicase: exploring the multifunctionality of an intriguing set of nonstructural proteins. Virus research 154:61-76
39. Feeley EM, Sims JS, John SP, Chin CR, Pertel T, Chen LM, Gaiha GD, Ryan BJ, Donis RO, Elledge SJ, Brass AL (2011) IFITM3 inhibits influenza A virus infection by preventing cytosolic entry. PLoS pathogens 7:e1002337
40. Fong LG, Ng JK, Meta M, Coté N, Yang SH, Stewart CL, Sullivan T, Burghardt A, Majumdar S, Reue K, Bergo MO, Young SG (2004) Heterozygosity for Lmna deficiency eliminates the progeria-like phenotypes in Zmpste24-deficient mice. Proceedings of the National Academy of Sciences of the United States of America 101:18111-18116
41. Franz S, Pott F, Zillinger T, Schüler C, Dapa S, Fischer C, Passos V, Stenzel S, Chen F, Döhner K, Hartmann G, Sodeik B, Pessler F, Simmons G, Drexler JF, Goffinet C (2021) Human IFITM3 restricts chikungunya virus and Mayaro virus infection and is susceptible to virus-mediated counteraction. Life Science Alliance 4:e202000909
42. Friedman RL, Manly SP, McMahon M, Kerr IM, Stark GR (1984) Transcriptional and posttranscriptional regulation of interferon-induced gene expression in human cells. Cell 38:745-755
43. Fu B, Wang L, Li S, Dorf ME (2017) ZMPSTE24 defends against influenza and other pathogenic viruses. The Journal of Experimental Medicine 214:919
44. Gack MU, Albrecht RA, Urano T, Inn K-S, Huang IC, Carnero E, Farzan M, Inoue S, Jung JU, García-Sastre A (2009) Influenza A Virus NS1 Targets the Ubiquitin Ligase TRIM25 to Evade Recognition by the Host Viral RNA Sensor RIG-I. Cell host & microbe 5:439-449

45. Gerlach T, Hensen L, Matrosovich T, Bergmann J, Winkler M, Peteranderl C, Klenk HD, Weber F, Herold S, Pöhlmann S, Matrosovich M (2017) pH Optimum of Hemagglutinin-Mediated Membrane Fusion Determines Sensitivity of Influenza A Viruses to the Interferon-Induced Antiviral State and IFITMs. Journal of virology 91
46. Gordon S (2001) Homeostasis: a scavenger receptor for haemoglobin. Current biology : CB 11:R399-401
47. Gorman MJ, Poddar S, Farzan M, Diamond MS (2016) The Interferon-Stimulated Gene Ifitm3 Restricts West Nile Virus Infection and Pathogenesis. Journal of virology 90:8212-8225
48. Graversen JH, Madsen M, Moestrup SK (2002) CD163: a signal receptor scavenging haptoglobin-hemoglobin complexes from plasma. The international journal of biochemistry & cell biology 34:309-314
49. Gruenbaum Y, Margalit A, Goldman RD, Shumaker DK, Wilson KL (2005) The nuclear lamina comes of age. Nature Reviews Molecular Cell Biology 6:21-31
50. Guo R, Katz BB, Tomich JM, Gallagher T, Fang Y (2016) Porcine Reproductive and Respiratory Syndrome Virus Utilizes Nanotubes for Intercellular Spread. Journal of virology 90:5163-5175
51. Guo X, Steinkühler J, Marin M, Li X, Lu W, Dimova R, Melikyan GB (2020) Interferon-Induced Transmembrane Protein 3 Blocks Fusion of Diverse Enveloped Viruses by Locally Altering Mechanical Properties of Cell Membranes. bioRxiv:2020.2006.2025.171280
52. Haller O, Kochs G (2010) Human MxA Protein: An Interferon-Induced Dynamin-Like GTPase with Broad Antiviral Activity. Journal of Interferon & Cytokine Research 31:79-87
53. Han J, Wang Y, Faaberg KS (2006) Complete genome analysis of RFLP 184 isolates of porcine reproductive and respiratory syndrome virus. Virus research 122:175-182
54. Harrison SC (2005) Mechanism of membrane fusion by viral envelope proteins. Adv Virus Res 64:231-261
55. Hildebrandt ER, Arachea BT, Wiener MC, Schmidt WK (2016) Ste24p Mediates Proteolysis of Both Isoprenylated and Non-prenylated Oligopeptides. J Biol Chem 291:14185-14198
56. Hoffmann H-H, Schneider WM, Rice CM (2015) Interferons and viruses: an evolutionary arms race of molecular interactions. Trends in Immunology 36:124-138
57. Huang IC, Bailey CC, Weyer JL, Radoshitzky SR, Becker MM, Chiang JJ, Brass AL, Ahmed AA, Chi X, Dong L, Longobardi LE, Boltz D, Kuhn JH, Elledge SJ, Bavari S, Denison MR, Choe H, Farzan M (2011) Distinct patterns of IFITM-mediated restriction of filoviruses, SARS coronavirus, and influenza A virus. PLoS pathogens 7:e1001258
58. Isaacs A, Lindenmann J (1957) Virus interference. I. The interferon. Proceedings of the Royal Society of London Series B, Biological sciences 147:258-267
59. Ivanovic T, Choi JL, Whelan SP, van Oijen AM, Harrison SC (2013) Influenza-virus membrane fusion by cooperative fold-back of stochastically induced hemagglutinin intermediates. Elife 2:e00333-e00333

60. Ji L, Zhou X, Liang W, Liu J, Liu B (2017) Porcine Interferon Stimulated Gene 12a Restricts Porcine Reproductive and Respiratory Syndrome Virus Replication in MARC-145 Cells. Int J Mol Sci 18:1613
61. Jia R, Pan Q, Ding S, Rong L, Liu S-L, Geng Y, Qiao W, Liang C (2012) The N-terminal region of IFITM3 modulates its antiviral activity by regulating IFITM3 cellular localization. Journal of virology 86:13697-13707
62. Jia R, Xu F, Qian J, Yao Y, Miao C, Zheng Y-M, Liu S-L, Guo F, Geng Y, Qiao W, Liang C (2014) Identification of an endocytic signal essential for the antiviral action of IFITM3. Cellular Microbiology 16:1080-1093
63. Jiang D, Weidner JM, Qing M, Pan XB, Guo H, Xu C, Zhang X, Birk A, Chang J, Shi PY, Block TM, Guo JT (2010) Identification of five interferon-induced cellular proteins that inhibit west nile virus and dengue virus infections. Journal of virology 84:8332-8341
64. John SP, Chin CR, Perreira JM, Feeley EM, Aker AM, Savidis G, Smith SE, Elia AE, Everitt AR, Vora M, Pertel T, Elledge SJ, Kellam P, Brass AL (2013) The CD225 domain of IFITM3 is required for both IFITM protein association and inhibition of influenza A virus and dengue virus replication. Journal of virology 87:7837-7852
65. Jongeneel CV, Bouvier J, Bairoch A (1989) A unique signature identifies a family of zinc-dependent metallopeptidases. FEBS Letters 242:211-214
66. Kappes MA, Faaberg KS (2015) PRRSV structure, replication and recombination: Origin of phenotype and genotype diversity. Virology 479-480:475-486
67. Karniychuk UU, Geldhof M, Vanhee M, Van Doorsselaere J, Saveleva TA, Nauwynck HJ (2010) Pathogenesis and antigenic characterization of a new East European subtype 3 porcine reproductive and respiratory syndrome virus isolate. BMC Veterinary Research 6:30
68. Karniychuk UU, Nauwynck HJ (2013) Pathogenesis and prevention of placental and transplacental porcine reproductive and respiratory syndrome virus infection. Veterinary research 44:95
69. Katze MG, He Y, Gale M (2002) Viruses and interferon: a fight for supremacy. Nature Reviews Immunology 2:675-687
70. Kim HS, Kwang J, Yoon IJ, Joo HS, Frey ML (1993) Enhanced replication of porcine reproductive and respiratory syndrome (PRRS) virus in a homogeneous subpopulation of MA-104 cell line. Archives of virology 133:477-483
71. Kim JK, Fahad AM, Shanmukhappa K, Kapil S (2006) Defining the cellular target(s) of porcine reproductive and respiratory syndrome virus blocking monoclonal antibody 7G10. Journal of virology 80:689-696
72. Kirchhoff F (2010) Immune evasion and counteraction of restriction factors by HIV-1 and other primate lentiviruses. Cell host & microbe 8:55-67
73. Kreutz LC, Ackermann MR (1996) Porcine reproductive and respiratory syndrome virus enters cells through a low pH-dependent endocytic pathway. Virus research 42:137-147
74. Kreutz LC (1998) Cellular membrane factors are the major determinants of porcine reproductive and respiratory syndrome virus tropism. Virus research 53:121-128

75. Kumar A, Kim JH, Ranjan P, Metcalfe MG, Cao W, Mishina M, Gangappa S, Guo Z, Boyden ES, Zaki S, York I, García-Sastre A, Shaw M, Sambhara S (2017) Influenza virus exploits tunneling nanotubes for cell-to-cell spread. Scientific Reports 7:40360
76. Lager KM, Mengeling WL (1995) Pathogenesis of in utero infection in porcine fetuses with porcine reproductive and respiratory syndrome virus. Canadian journal of veterinary research = Revue canadienne de recherche veterinaire 59:187-192
77. Lam JKW, Chow MYT, Zhang Y, Leung SWS (2015) siRNA Versus miRNA as Therapeutics for Gene Silencing. Molecular Therapy - Nucleic Acids 4:e252
78. Larner AC, Chaudhuri A, Darnell JE (1986) Transcriptional induction by interferon. New protein(s) determine the extent and length of the induction. Journal of Biological Chemistry 261:453-459
79. Lei C, Yang J, Hu J, Sun X (2021) On the Calculation of TCID(50) for Quantitation of Virus Infectivity. Virol Sin 36:141-144
80. Lengyel P (1982) Biochemistry of Interferons and Their Actions. Annual Review of Biochemistry 51:251-282
81. Levy DE, Garcı, x, a-Sastre A (2001) The virus battles: IFN induction of the antiviral state and mechanisms of viral evasion. Cytokine & Growth Factor Reviews 12:143-156
82. Li C, Zheng H, Wang Y, Dong W, Liu Y, Zhang L, Zhang Y (2019) Antiviral Role of IFITM Proteins in Classical Swine Fever Virus Infection. Viruses 11:126
83. Li K, Markosyan RM, Zheng Y-M, Golfetto O, Bungart B, Li M, Ding S, He Y, Liang C, Lee JC, Gratton E, Cohen FS, Liu S-L (2013) IFITM proteins restrict viral membrane hemifusion. PLoS pathogens 9:e1003124-e1003124
84. Li S, Fu B, Wang L, Dorf ME (2017) ZMPSTE24 Is Downstream Effector of Interferon-Induced Transmembrane Antiviral Activity. DNA Cell Biol 36:513-517
85. Li Y, Li C, Xue P, Zhong B, Mao A-P, Ran Y, Chen H, Wang Y-Y, Yang F, Shu H-B (2009) ISG56 is a negative-feedback regulator of virus-triggered signaling and cellular antiviral response. Proceedings of the National Academy of Sciences 106:7945
86. Lin TY, Chin CR, Everitt AR, Clare S, Perreira JM, Savidis G, Aker AM, John SP, Sarlah D, Carreira EM, Elledge SJ, Kellam P, Brass AL (2013) Amphotericin B increases influenza A virus infection by preventing IFITM3-mediated restriction. Cell reports 5:895-908
87. Liu Y-J (2004) IPC: Professional Type 1 Interferon-Producing Cells and Plasmacytoid Dendritic Cell Precursors. Annual review of immunology 23:275-306
88. Livak KJ, Schmittgen TD (2001) Analysis of Relative Gene Expression Data Using Real-Time Quantitative PCR and the 2−ΔΔCT Method. Methods 25:402-408
89. Loving CL, Osorio FA, Murtaugh MP, Zuckermann FA (2015) Innate and adaptive immunity against Porcine Reproductive and Respiratory Syndrome Virus. Veterinary Immunology and Immunopathology 167:1-14

90. Lunney JK, Fang Y, Ladinig A, Chen N, Li Y, Rowland B, Renukaradhya GJ (2016) Porcine Reproductive and Respiratory Syndrome Virus (PRRSV): Pathogenesis and Interaction with the Immune System. Annual review of animal biosciences 4:129-154
91. McMichael TM, Zhang Y, Kenney AD, Zhang L, Zani A, Lu M, Chemudupati M, Li J, Yount JS (2018) IFITM3 Restricts Human Metapneumovirus Infection. The Journal of infectious diseases 218:1582-1591
92. Mellman I, Fuchs R, Helenius A (1986) Acidification of the endocytic and exocytic pathways. Annu Rev Biochem 55:663-700
93. Mengeling WL, Lager KM, Vorwald AC (1998) Clinical consequences of exposing pregnant gilts to strains of porcine reproductive and respiratory syndrome (PRRS) virus isolated from field cases of "atypical" PRRS. American journal of veterinary research 59:1540-1544
94. Michaelis S, Barrowman J (2012) Biogenesis of the Saccharomyces cerevisiae pheromone a-factor, from yeast mating to human disease. Microbiol Mol Biol Rev 76:626-651
95. Munir M, Berg M (2013) The multiple faces of proteinkinase R in antiviral defense. Virulence 4:85-89
96. Nauwynck HJ, Duan X, Favoreel HW, Van Oostveldt P, Pensaert MB (1999) Entry of porcine reproductive and respiratory syndrome virus into porcine alveolar macrophages via receptor-mediated endocytosis. The Journal of general virology 80 (Pt 2):297-305
97. Nelsen CJ, Murtaugh MP, Faaberg KS (1999) Porcine reproductive and respiratory syndrome virus comparison: divergent evolution on two continents. Journal of virology 73:270-280
98. Nelson EA, Christopher-Hennings J, Drew T, Wensvoort G, Collins JE, Benfield DA (1993) Differentiation of U.S. and European isolates of porcine reproductive and respiratory syndrome virus by monoclonal antibodies. Journal of clinical microbiology 31:3184-3189
99. Okumura F, Okumura AJ, Uematsu K, Hatakeyama S, Zhang DE, Kamura T (2013) Activation of double-stranded RNA-activated protein kinase (PKR) by interferon-stimulated gene 15 (ISG15) modification down-regulates protein translation. J Biol Chem 288:2839-2847
100. Ostrowski M, Galeota JA, Jar AM, Platt KB, Osorio FA, Lopez OJ (2002) Identification of neutralizing and nonneutralizing epitopes in the porcine reproductive and respiratory syndrome virus GP5 ectodomain. Journal of virology 76:4241-4250
101. Panasiuk M, Rychłowski M, Derewońko N, Bieńkowska-Szewczyk K (2018) Tunneling Nanotubes as a Novel Route of Cell-to-Cell Spread of Herpesviruses. Journal of virology 92
102. Patel D, Nan Y, Shen M, Ritthipichai K, Zhu X, Zhang Y-J (2010) Porcine Reproductive and Respiratory Syndrome Virus Inhibits Type I Interferon Signaling by Blocking STAT1/STAT2 Nuclear Translocation. Journal of virology 84:11045
103. Pedersen KW, van der Meer Y, Roos N, Snijder EJ (1999) Open Reading Frame 1a-Encoded Subunits of the Arterivirus Replicase Induce Endoplasmic

Reticulum-Derived Double-Membrane Vesicles Which Carry the Viral Replication Complex. Journal of virology 73:2016

104. Perreira JM, Chin CR, Feeley EM, Brass AL (2013) IFITMs Restrict the Replication of Multiple Pathogenic Viruses. Journal of Molecular Biology 425:4937-4955
105. Pileri E, Mateu E (2016) Review on the transmission porcine reproductive and respiratory syndrome virus between pigs and farms and impact on vaccination. Veterinary research 47:108
106. Pryor EE, Jr., Horanyi PS, Clark KM, Fedoriw N, Connelly SM, Koszelak-Rosenblum M, Zhu G, Malkowski MG, Wiener MC, Dumont ME (2013) Structure of the integral membrane protein CAAX protease Ste24p. Science (New York, NY) 339:1600-1604
107. Quigley A, Dong YY, Pike ACW, Dong L, Shrestha L, Berridge G, Stansfeld PJ, Sansom MSP, Edwards AM, Bountra C, von Delft F, Bullock AN, Burgess-Brown NA, Carpenter EP (2013) The Structural Basis of ZMPSTE24-Dependent Laminopathies. Science (New York, NY) 339:1604
108. Rowland RR, Robinson B, Stefanick J, Kim TS, Guanghua L, Lawson SR, Benfield DA (2001) Inhibition of porcine reproductive and respiratory syndrome virus by interferon-gamma and recovery of virus replication with 2-aminopurine. Archives of virology 146:539-555
109. Samuel CE (2001) Antiviral actions of interferons. Clinical microbiology reviews 14:778-809
110. Sánchez-Torres C, Gómez-Puertas P, Gómez-del-Moral M, Alonso F, Escribano JM, Ezquerra A, Domínguez J (2003) Expression of porcine CD163 on monocytes/macrophages correlates with permissiveness to African swine fever infection. Archives of virology 148:2307-2323
111. Sánchez C, Doménech N, Vázquez J, Alonso F, Ezquerra A, Domínguez J (1999) The porcine 2A10 antigen is homologous to human CD163 and related to macrophage differentiation. Journal of immunology (Baltimore, Md : 1950) 162:5230-5237
112. Savidis G, Perreira Jill M, Portmann Jocelyn M, Meraner P, Guo Z, Green S, Brass Abraham L (2016) The IFITMs Inhibit Zika Virus Replication. Cell reports 15:2323-2330
113. Schindelin J, Arganda-Carreras I, Frise E, Kaynig V, Longair M, Pietzsch T, Preibisch S, Rueden C, Saalfeld S, Schmid B, Tinevez J-Y, White DJ, Hartenstein V, Eliceiri K, Tomancak P, Cardona A (2012) Fiji: an open-source platform for biological-image analysis. Nature Methods 9:676-682
114. Schneider CA, Rasband WS, Eliceiri KW (2012) NIH Image to ImageJ: 25 years of image analysis. Nature Methods 9:671-675
115. Schneider WM, Chevillotte MD, Rice CM (2014) Interferon-stimulated genes: a complex web of host defenses. Annual review of immunology 32:513-545
116. Schoggins JW, Rice CM (2011) Interferon-stimulated genes and their antiviral effector functions. Current opinion in virology 1:519-525
117. Schoggins JW, Wilson SJ, Panis M, Murphy MY, Jones CT, Bieniasz P, Rice CM (2011) A diverse range of gene products are effectors of the type I interferon antiviral response. Nature 472:481-485

118. Shi C, Liu Y, Ding Y, Zhang Y, Zhang J (2015) PRRSV receptors and their roles in virus infection. Archives of Microbiology 197:503-512
119. Shi G, Schwartz O, Compton AA (2017) More than meets the I: the diverse antiviral and cellular functions of interferon-induced transmembrane proteins. Retrovirology 14:53
120. Sieczkarski SB, Whittaker GR (2005) Viral entry. Current topics in microbiology and immunology 285:1-23
121. Smith S, Weston S, Kellam P, Marsh M (2014) IFITM proteins-cellular inhibitors of viral entry. Current opinion in virology 4:71-77
122. Spear ED, Alford RF, Babatz TD, Wood KM, Mossberg OW, Odinammadu K, Shilagardi K, Gray JJ, Michaelis S (2019) A humanized yeast system to analyze cleavage of prelamin A by ZMPSTE24. Methods 157:47-55
123. Stott RJ, Foster TL (2021) Inhibition of arenavirus entry and replication by the cell-intrinsic restriction factor ZMPSTE24 is enhanced by IFITM antiviral activity. bioRxiv:2021.2004.2012.439453
124. Suddala KC, Lee CC, Meraner P, Marin M, Markosyan RM, Desai TM, Cohen FS, Brass AL, Melikyan GB (2019) Interferon-induced transmembrane protein 3 blocks fusion of sensitive but not resistant viruses by partitioning into virus-carrying endosomes. PLoS pathogens 15:e1007532
125. Takeuchi O, Akira S (2010) Pattern recognition receptors and inflammation. Cell 140:805-820
126. tenOever BR (2016) The Evolution of Antiviral Defense Systems. Cell host & microbe 19:142-149
127. Therrien D, St-Pierre Y, Dea S (2000) Preliminary characterization of protein binding factor for porcine reproductive and respiratory syndrome virus on the surface of permissive and non-permissive cells. Archives of virology 145:1099-1116
128. Tian K, Yu X, Zhao T, Feng Y, Cao Z, Wang C, Hu Y, Chen X, Hu D, Tian X, Liu D, Zhang S, Deng X, Ding Y, Yang L, Zhang Y, Xiao H, Qiao M, Wang B, Hou L, Wang X, Yang X, Kang L, Sun M, Jin P, Wang S, Kitamura Y, Yan J, Gao GF (2007) Emergence of fatal PRRSV variants: unparalleled outbreaks of atypical PRRS in China and molecular dissection of the unique hallmark. PloS one 2:e526
129. Van Breedam W, Verbeeck M, Christiaens I, Van Gorp H, Nauwynck HJ (2013) Porcine, murine and human sialoadhesin (Sn/Siglec-1/CD169): portals for porcine reproductive and respiratory syndrome virus entry into target cells. The Journal of general virology 94:1955-1960
130. Van Gorp H, Van Breedam W, Delputte PL, Nauwynck HJ (2008) Sialoadhesin and CD163 join forces during entry of the porcine reproductive and respiratory syndrome virus. The Journal of general virology 89:2943-2953
131. Van Gorp H, Van Breedam W, Delputte PL, Nauwynck HJ (2009) The porcine reproductive and respiratory syndrome virus requires trafficking through CD163-positive early endosomes, but not late endosomes, for productive infection. Archives of virology 154:1939-1943
132. Van Gorp H, Van Breedam W, Van Doorsselaere J, Delputte PL, Nauwynck HJ (2010) Identification of the CD163 Protein Domains Involved in Infection of the

Porcine Reproductive and Respiratory Syndrome Virus. Journal of virology 84:3101

133. van Nieuwstadt AP, Meulenberg JJ, van Essen-Zanbergen A, Petersen-den Besten A, Bende RJ, Moormann RJ, Wensvoort G (1996) Proteins encoded by open reading frames 3 and 4 of the genome of Lelystad virus (Arteriviridae) are structural proteins of the virion. Journal of virology 70:4767-4772
134. Van Reeth K, Labarque G, Nauwynck H, Pensaert M (1999) Differential production of proinflammatory cytokines in the pig lung during different respiratory virus infections: correlations with pathogenicity. Research in veterinary science 67:47-52
135. Vanderheijden N, Delputte PL, Favoreel HW, Vandekerckhove J, Van Damme J, van Woensel PA, Nauwynck HJ (2003) Involvement of sialoadhesin in entry of porcine reproductive and respiratory syndrome virus into porcine alveolar macrophages. Journal of virology 77:8207-8215
136. Verhelst J, Hulpiau P, Saelens X (2013) Mx proteins: antiviral gatekeepers that restrain the uninvited. Microbiol Mol Biol Rev 77:551-566
137. Vu HL, Kwon B, Yoon KJ, Laegreid WW, Pattnaik AK, Osorio FA (2011) Immune evasion of porcine reproductive and respiratory syndrome virus through glycan shielding involves both glycoprotein 5 as well as glycoprotein 3. Journal of virology 85:5555-5564
138. Waheed AA, Ablan SD, Soheilian F, Nagashima K, Ono A, Schaffner CP, Freed EO (2008) Inhibition of human immunodeficiency virus type 1 assembly and release by the cholesterol-binding compound amphotericin B methyl ester: evidence for Vpu dependence. Journal of virology 82:9776-9781
139. Wang JT, Doong SL, Teng SC, Lee CP, Tsai CH, Chen MR (2009) Epstein-Barr virus BGLF4 kinase suppresses the interferon regulatory factor 3 signaling pathway. Journal of virology 83:1856-1869
140. Wang X, Zhang H, Abel AM, Nelson E (2016) Protein kinase R (PKR) plays a pro-viral role in porcine reproductive and respiratory syndrome virus (PRRSV) replication by modulating viral gene transcription. Archives of virology 161:327-333
141. Wee YS, Roundy KM, Weis JJ, Weis JH (2012) Interferon-inducible transmembrane proteins of the innate immune response act as membrane organizers by influencing clathrin and v-ATPase localization and function. Innate immunity 18:834-845
142. Weidner JM, Jiang D, Pan XB, Chang J, Block TM, Guo JT (2010) Interferon-induced cell membrane proteins, IFITM3 and tetherin, inhibit vesicular stomatitis virus infection via distinct mechanisms. Journal of virology 84:12646-12657
143. Weiss CM, Trobaugh DW, Sun C, Lucas TM, Diamond MS, Ryman KD, Klimstra WB (2018) The Interferon-Induced Exonuclease ISG20 Exerts Antiviral Activity through Upregulation of Type I Interferon Response Proteins. mSphere 3
144. Welch SK, Calvert JG (2010) A brief review of CD163 and its role in PRRSV infection. Virus research 154:98-103
145. Wensvoort G, Terpstra C, Pol JM, ter Laak EA, Bloemraad M, de Kluyver EP, Kragten C, van Buiten L, den Besten A, Wagenaar F, et al. (1991) Mystery swine

disease in The Netherlands: the isolation of Lelystad virus. The veterinary quarterly 13:121-130
146. Williams BR (1999) PKR; a sentinel kinase for cellular stress. Oncogene 18:6112-6120
147. Wyles JP, McMaster CR, Ridgway ND (2002) Vesicle-associated membrane protein-associated protein-A (VAP-A) interacts with the oxysterol-binding protein to modify export from the endoplasmic reticulum. J Biol Chem 277:29908-29918
148. Xiao Y, Ma Z, Wang R, Yang L, Nan Y, Zhang YJ (2016) Downregulation of protein kinase PKR activation by porcine reproductive and respiratory syndrome virus at its early stage infection. Veterinary microbiology 187:1-7
149. Yoon KJ, Wu LL, Zimmerman JJ, Hill HT, Platt KB (1996) Antibody-dependent enhancement (ADE) of porcine reproductive and respiratory syndrome virus (PRRSV) infection in pigs. Viral immunology 9:51-63
150. Yount JS, Moltedo B, Yang YY, Charron G, Moran TM, López CB, Hang HC (2010) Palmitoylome profiling reveals S-palmitoylation-dependent antiviral activity of IFITM3. Nature chemical biology 6:610-614
151. Yount JS, Karssemeijer RA, Hang HC (2012) S-palmitoylation and ubiquitination differentially regulate interferon-induced transmembrane protein 3 (IFITM3)-mediated resistance to influenza virus. J Biol Chem 287:19631-19641
152. Zerial M, McBride H (2001) Rab proteins as membrane organizers. Nature Reviews Molecular Cell Biology 2:107-117
153. Zhang A, Duan H, Zhao H, Liao H, Du Y, Li L, Jiang D, Wan B, Wu Y, Ji P, Zhou E-M, Zhang G (2020) Interferon-Induced Transmembrane Protein 3 Is a Virus-Associated Protein Which Suppresses Porcine Reproductive and Respiratory Syndrome Virus Replication by Blocking Viral Membrane Fusion. Journal of virology 94:e01350-01320
154. Zhang APP, Abelson DM, Bornholdt ZA, Liu T, Woods VL, Jr., Saphire EO (2012) The ebolavirus VP24 interferon antagonist: know your enemy. Virulence 3:440-445
155. Zhang H, Guo X, Nelson E, Christopher-Hennings J, Wang X (2012) Porcine reproductive and respiratory syndrome virus activates the transcription of interferon alpha/beta (IFN-α/β) in monocyte-derived dendritic cells (Mo-DC). Veterinary microbiology 159:494-498
156. Zhang Q, Yoo D (2015) PRRS virus receptors and their role for pathogenesis. Veterinary microbiology 177:229-241
157. Zhao X, Guo F, Liu F, Cuconati A, Chang J, Block TM, Guo JT (2014) Interferon induction of IFITM proteins promotes infection by human coronavirus OC43. Proceedings of the National Academy of Sciences of the United States of America 111:6756-6761
158. Zhao X, Zheng S, Chen D, Zheng M, Li X, Li G, Lin H, Chang J, Zeng H, Guo JT (2020) LY6E Restricts Entry of Human Coronaviruses, Including Currently Pandemic SARS-CoV-2. Journal of virology 94
159. Zhou A, Paranjape JM, Der SD, Williams BR, Silverman RH (1999) Interferon action in triply deficient mice reveals the existence of alternative antiviral pathways. Virology 258:435-440

160. Zhou Z, Wang N, Woodson SE, Dong Q, Wang J, Liang Y, Rijnbrand R, Wei L, Nichols JE, Guo JT, Holbrook MR, Lemon SM, Li K (2011) Antiviral activities of ISG20 in positive-strand RNA virus infections. Virology 409:175-188
161. Zimmerman JJ, Yoon KJ, Wills RW, Swenson SL (1997) General overview of PRRSV: a perspective from the United States. Veterinary microbiology 55:187-196